A RESIDUAL BASED *A POSTERIORI* ERROR ESTIMATOR FOR AN AUGMENTED MIXED FINITE ELEMENT METHOD IN LINEAR ELASTICITY [*]

Tomás P. Barrios[1], Gabriel N. Gatica[2], María González[3] and Norbert Heuer[4]

Abstract. In this paper we develop a residual based *a posteriori* error analysis for an augmented mixed finite element method applied to the problem of linear elasticity in the plane. More precisely, we derive a reliable and efficient *a posteriori* error estimator for the case of pure Dirichlet boundary conditions. In addition, several numerical experiments confirming the theoretical properties of the estimator, and illustrating the capability of the corresponding adaptive algorithm to localize the singularities and the large stress regions of the solution, are also reported.

Mathematics Subject Classification. 65N15, 65N30, 65N50, 74B05.

Received: November 9, 2005.

1. Introduction

A new stabilized mixed finite element method for plane linear elasticity was presented and analyzed recently in [10]. The approach there is based on the introduction of suitable Galerkin least-squares terms arising from the constitutive and equilibrium equations, and from the relation defining the rotation in terms of the displacement. The resulting augmented method, which is easily generalized to 3D, can be viewed as an extension to the elasticity problem of the non-symmetric procedures utilized in [8] and [11]. It is shown in [10] that the continuous and discrete augmented formulations are well-posed, and that the latter becomes locking-free and asymptotically locking-free for Dirichlet and mixed boundary conditions, respectively. Moreover, the augmented variational formulation introduced in [10], being strongly coercive in the case of Dirichlet boundary conditions, allows the utilization of arbitrary finite element subspaces for the corresponding discrete scheme, which constitutes one of its main advantages. In particular, Raviart-Thomas spaces of lowest order for the stress tensor, piecewise linear elements for the displacement, and piecewise constants for the rotation can be used. In the case of mixed boundary conditions, the essential one (Neumann) is imposed weakly, which yields the introduction of

[1] Facultad de Ingeniería, Universidad Católica de la Santísima Concepción, Casilla 297, Concepción, Chile. `tomas@ucsc.cl`

[2] GI²MA, Departamento de Ingeniería Matemática, Universidad de Concepción, Casilla 160-C, Concepción, Chile. `ggatica@ing-mat.udec.cl`

[3] Departamento de Matemáticas, Universidade da Coruña, Campus de Elviña s/n, 15071 A Coruña, Spain. `mgtaboad@udc.es`

[4] BICOM and Department of Mathematical Sciences, Brunel University, Uxbridge, UB8 3PH, UK. `norbert.heuer@brunel.ac.uk`

the trace of the displacement as a suitable Lagrange multiplier. This trace is then approximated by piecewise linear elements on an independent partition of the Neumann boundary whose mesh size needs to satisfy a compatibility condition with the mesh size associated with the triangulation of the domain. Further details on the advantages of the augmented method can be found in [10] and also throughout the present paper (see, in particular, Sect. 5 below).

According to the above, and strongly motivated by the competitive character of our augmented formulation, we now feel the need of deriving corresponding *a posteriori* error estimators. More precisely, the purpose of this work is to develop a residual based *a posteriori* error analysis for the augmented mixed finite element scheme from [10] in the case of pure Dirichlet boundary conditions. *A posteriori* error analyses of the traditional mixed finite element methods for the elasticity problem can be seen in [5] and the references therein. The rest of this paper is organized as follows. In Section 2 we recall from [10] the continuous and discrete augmented formulations of the corresponding boundary value problem, state the well-posedness of both schemes, and provide the associated *a priori* error estimate. The kernel of the present work is given by Sections 3 and 4, where we develop the residual based *a posteriori* error analysis. Indeed, in Section 3 we employ a suitable auxiliary problem and apply integration by parts and the local approximation properties of the Clément interpolant to derive a reliable *a posteriori* error estimator. In other words, the method that we use to prove reliability combines a technique utilized in mixed finite element schemes with the usual procedure applied to primal finite element methods. It is important to remark that just one of these approaches by itself would not be enough in this case. In addition, up to our knowledge, this combined analysis seems to be applied here for the first time. Next, in Section 4 we make use of inverse inequalities and the localization technique based on triangle-bubble and edge-bubble functions to show that the estimator is efficient. We remark that, because of the new Galerkin least-squares terms employed, most of the residual terms defining the error indicator are new, and hence our proof of efficiency needs to previously establish more general versions of some technical lemmas concerning inverse estimates and piecewise polynomials. Finally, several numerical results confirming reliability, efficiency, and robustness of the estimator with respect to the Poisson ratio, are provided in Section 5. In addition, the capability of the corresponding adaptive algorithm to localize the singularities and the large stress regions of the solution is also illustrated here.

We end this section with some notations to be used below. Given any Hilbert space U, U^2 and $U^{2\times2}$ denote, respectively, the space of vectors and square matrices of order 2 with entries in U. In addition, $\mathbf{I}$ is the identity matrix of $\mathbb{R}^{2\times2}$, and given $\boldsymbol{\tau} := (\tau_{ij})$, $\boldsymbol{\zeta} := (\zeta_{ij}) \in \mathbb{R}^{2\times2}$, we write as usual

$$\boldsymbol{\tau}^{\mathrm{t}} := (\tau_{ji}), \quad \mathrm{tr}(\boldsymbol{\tau}) := \sum_{i=1}^{2} \tau_{ii}, \quad \boldsymbol{\tau}^{\mathrm{d}} := \boldsymbol{\tau} - \frac{1}{2}\mathrm{tr}(\boldsymbol{\tau})\,\mathbf{I}, \quad \text{and} \quad \boldsymbol{\tau}:\boldsymbol{\zeta} := \sum_{i,j=1}^{2} \tau_{ij}\,\zeta_{ij}\,.$$

Also, in what follows we utilize the standard terminology for Sobolev spaces and norms, employ $\mathbf{0}$ to denote a generic null vector, and use C and c, with or without subscripts, bars, tildes or hats, to denote generic constants independent of the discretization parameters, which may take different values at different places.

2. THE AUGMENTED FORMULATIONS

First we let Ω be a simply connected domain in $\mathbb{R}^2$ with polygonal boundary $\Gamma := \partial\Omega$. Our goal is to determine the displacement $\mathbf{u}$ and stress tensor $\boldsymbol{\sigma}$ of a linear elastic material occupying the region Ω. In other words, given a volume force $\mathbf{f} \in [L^2(\Omega)]^2$, we seek a symmetric tensor field $\boldsymbol{\sigma}$ and a vector field $\mathbf{u}$ such that

$$\boldsymbol{\sigma} = \mathcal{C}\,\mathbf{e}(\mathbf{u}), \quad \mathbf{div}(\boldsymbol{\sigma}) = -\,\mathbf{f} \quad \text{in} \quad \Omega\,, \quad \text{and} \quad \mathbf{u} = \mathbf{0} \quad \text{on} \quad \Gamma\,. \tag{1}$$

Hereafter, $\mathbf{e}(\mathbf{u}) := \frac{1}{2}\left(\nabla\mathbf{u} + (\nabla\mathbf{u})^{\mathrm{t}}\right)$ is the strain tensor of small deformations and $\mathcal{C}$ is the elasticity tensor

determined by Hooke's law, that is

$$\mathcal{C}\,\boldsymbol{\zeta} \; := \; \lambda\,\mathrm{tr}(\boldsymbol{\zeta})\,\mathbf{I} \; + \; 2\,\mu\,\boldsymbol{\zeta} \qquad \forall\,\boldsymbol{\zeta} \in [L^2(\Omega)]^{2\times 2}\,, \tag{2}$$

where $\lambda,\,\mu > 0$ denote the corresponding Lamé constants. It is easy to see from (2) that the inverse tensor $\mathcal{C}^{-1}$ reduces to

$$\mathcal{C}^{-1}\,\boldsymbol{\zeta} \; := \; \frac{1}{2\,\mu}\,\boldsymbol{\zeta} \; - \; \frac{\lambda}{4\,\mu\,(\lambda+\mu)}\,\mathrm{tr}(\boldsymbol{\zeta})\,\mathbf{I} \qquad \forall\,\boldsymbol{\zeta} \in [L^2(\Omega)]^{2\times 2}\,. \tag{3}$$

We now define the spaces $H = H(\mathbf{div}\,;\Omega) := \{\boldsymbol{\tau} \in [L^2(\Omega)]^{2\times 2} : \quad \mathbf{div}(\boldsymbol{\tau}) \in [L^2(\Omega)]^2\}$, $H_0 := \{\boldsymbol{\tau} \in H : \int_\Omega \mathrm{tr}(\boldsymbol{\tau}) = 0\}$, and note that $H = H_0 \oplus \mathbb{R}\,\mathbf{I}$, that is for any $\boldsymbol{\tau} \in H$ there exist unique $\boldsymbol{\tau}_0 \in H_0$ and $d := \frac{1}{2|\Omega|}\int_\Omega \mathrm{tr}(\boldsymbol{\tau}) \in \mathbb{R}$ such that $\boldsymbol{\tau} = \boldsymbol{\tau}_0 + d\,\mathbf{I}$. In addition, we define the space of skew-symmetric tensors $[L^2(\Omega)]^{2\times 2}_{\mathtt{skew}} := \{\boldsymbol{\eta} \in [L^2(\Omega)]^{2\times 2} : \boldsymbol{\eta}+\boldsymbol{\eta}^{\mathtt{t}} = \mathbf{0}\}$ and introduce the rotation $\boldsymbol{\gamma} := \frac{1}{2}(\nabla\mathbf{u}-(\nabla\mathbf{u})^{\mathtt{t}})) \in [L^2(\Omega)]^{2\times 2}_{\mathtt{skew}}$ as an auxiliary unknown. Then, given positive parameters κ_1, κ_2, and κ_3, independent of λ, we consider from [10] the following augmented variational formulation for (1): Find $(\boldsymbol{\sigma},\mathbf{u},\boldsymbol{\gamma}) \in \mathbf{H}_0 := H_0 \times [H^1_0(\Omega)]^2 \times [L^2(\Omega)]^{2\times 2}_{\mathtt{skew}}$ such that

$$A((\boldsymbol{\sigma},\mathbf{u},\boldsymbol{\gamma}),(\boldsymbol{\tau},\mathbf{v},\boldsymbol{\eta})) \; = \; F(\boldsymbol{\tau},\mathbf{v},\boldsymbol{\eta}) \qquad \forall\,(\boldsymbol{\tau},\mathbf{v},\boldsymbol{\eta}) \in \mathbf{H}_0\,, \tag{4}$$

where the bilinear form $A : \mathbf{H}_0 \times \mathbf{H}_0 \to \mathbb{R}$ and the functional $F : \mathbf{H}_0 \to \mathbb{R}$ are defined by

$$A((\boldsymbol{\sigma},\mathbf{u},\boldsymbol{\gamma}),(\boldsymbol{\tau},\mathbf{v},\boldsymbol{\eta})) := \int_\Omega \mathcal{C}^{-1}\boldsymbol{\sigma} : \boldsymbol{\tau} + \int_\Omega \mathbf{u}\cdot\mathbf{div}(\boldsymbol{\tau}) + \int_\Omega \boldsymbol{\gamma} : \boldsymbol{\tau} - \int_\Omega \mathbf{v}\cdot\mathbf{div}(\boldsymbol{\sigma}) - \int_\Omega \boldsymbol{\eta} : \boldsymbol{\sigma}$$

$$+ \; \kappa_1 \int_\Omega \big(\mathbf{e}(\mathbf{u}) - \mathcal{C}^{-1}\boldsymbol{\sigma}\big) : \big(\mathbf{e}(\mathbf{v}) + \mathcal{C}^{-1}\boldsymbol{\tau}\big) \; + \; \kappa_2 \int_\Omega \mathbf{div}(\boldsymbol{\sigma})\cdot\mathbf{div}(\boldsymbol{\tau})$$

$$+ \; \kappa_3 \int_\Omega \left(\boldsymbol{\gamma} - \frac{1}{2}(\nabla\mathbf{u} - (\nabla\mathbf{u})^{\mathtt{t}})\right) : \left(\boldsymbol{\eta} + \frac{1}{2}(\nabla\mathbf{v} - (\nabla\mathbf{v})^{\mathtt{t}})\right)\,, \tag{5}$$

and

$$F(\boldsymbol{\tau},\mathbf{v},\boldsymbol{\eta}) \; := \; \int_\Omega \mathbf{f}\cdot(\mathbf{v} - \kappa_2\,\mathbf{div}(\boldsymbol{\tau}))\,. \tag{6}$$

The well-posedness of (4) was proved in [10]. More precisely, we have the following result.

Theorem 2.1. *Assume that $(\kappa_1,\kappa_2,\kappa_3)$ is independent of λ and such that $0 < \kappa_1 < 2\,\mu$, $0 < \kappa_2$, and $0 < \kappa_3 < \kappa_1$. Then, there exist positive constants M, α, independent of λ, such that*

$$|\,A((\boldsymbol{\sigma},\mathbf{u},\boldsymbol{\gamma}),(\boldsymbol{\tau},\mathbf{v},\boldsymbol{\eta}))\,| \; \leq \; M\,\|(\boldsymbol{\sigma},\mathbf{u},\boldsymbol{\gamma})\|_{\mathbf{H}_0}\,\|(\boldsymbol{\tau},\mathbf{v},\boldsymbol{\eta})\|_{\mathbf{H}_0} \tag{7}$$

and

$$A((\boldsymbol{\tau},\mathbf{v},\boldsymbol{\eta}),(\boldsymbol{\tau},\mathbf{v},\boldsymbol{\eta})) \; \geq \; \alpha\,\|(\boldsymbol{\tau},\mathbf{v},\boldsymbol{\eta})\|^2_{\mathbf{H}_0} \tag{8}$$

for all $(\boldsymbol{\sigma},\mathbf{u},\boldsymbol{\gamma})$, $(\boldsymbol{\tau},\mathbf{v},\boldsymbol{\eta}) \in \mathbf{H}_0$. In particular, taking

$$\kappa_1 = \tilde{C}_1\,\mu, \qquad \kappa_2 = \frac{1}{\mu}\left(1 - \frac{\kappa_1}{2\,\mu}\right), \qquad and \qquad \kappa_3 = \tilde{C}_3\,\kappa_1\,, \tag{9}$$

with any $\tilde{C}_1 \in\,]0,2[$ and any $\tilde{C}_3 \in\,]0,1[$, this yields M and α depending only on μ, $\frac{1}{\mu}$, and Ω. Therefore, the augmented variational formulation (4) has a unique solution $(\boldsymbol{\sigma},\mathbf{u},\boldsymbol{\gamma}) \in \mathbf{H}_0$, and there exists a positive constant C, independent of λ, such that

$$\|(\boldsymbol{\sigma},\mathbf{u},\boldsymbol{\gamma})\|_{\mathbf{H}_0} \; \leq \; C\,\|F\| \; \leq \; C\,\|\mathbf{f}\|_{[L^2(\Omega)]^2}\,.$$

Proof. See Theorems 3.1 and 3.2 in [10]. $\qquad\square$

Now, given a finite element subspace $\mathbf{H}_{0,h} \subseteq \mathbf{H}_0$, the Galerkin scheme associated with (4) reads: Find $(\boldsymbol{\sigma}_h, \mathbf{u}_h, \boldsymbol{\gamma}_h) \in \mathbf{H}_{0,h}$ such that

$$A((\boldsymbol{\sigma}_h, \mathbf{u}_h, \boldsymbol{\gamma}_h), (\boldsymbol{\tau}_h, \mathbf{v}_h, \boldsymbol{\eta}_h)) = F(\boldsymbol{\tau}_h, \mathbf{v}_h, \boldsymbol{\eta}_h) \qquad \forall (\boldsymbol{\tau}_h, \mathbf{v}_h, \boldsymbol{\eta}_h) \in \mathbf{H}_{0,h}, \tag{10}$$

where κ_1, κ_2, and κ_3, being the same parameters employed in the formulation (4), satisfy the assumptions of Theorem 2.1. Since A becomes bounded and strongly coercive on the whole space $\mathbf{H}_0$, we remark that the well posedness of (10) is guaranteed for any arbitrary choice of the subspace $\mathbf{H}_{0,h}$. In fact, the following result is also established in [10].

Theorem 2.2. *Assume that the parameters κ_1, κ_2, and κ_3 satisfy the assumptions of Theorem 2.1 and let $\mathbf{H}_{0,h}$ be any finite element subspace of $\mathbf{H}_0$. Then, the Galerkin scheme (10) has a unique solution $(\boldsymbol{\sigma}_h, \mathbf{u}_h, \boldsymbol{\gamma}_h) \in \mathbf{H}_{0,h}$, and there exist positive constants C, $\tilde{C}$, independent of h and λ, such that*

$$\|(\boldsymbol{\sigma}_h, \mathbf{u}_h, \boldsymbol{\gamma}_h)\|_{\mathbf{H}_0} \leq C \sup_{\substack{(\boldsymbol{\tau}_h, \mathbf{v}_h, \boldsymbol{\eta}_h) \in \mathbf{H}_{0,h} \\ (\boldsymbol{\tau}_h, \mathbf{v}_h, \boldsymbol{\eta}_h) \neq \mathbf{0}}} \frac{|F(\boldsymbol{\tau}_h, \mathbf{v}_h, \boldsymbol{\eta}_h)|}{\|(\boldsymbol{\tau}_h, \mathbf{v}_h, \boldsymbol{\eta}_h)\|_{\mathbf{H}_0}} \leq C \|\mathbf{f}\|_{[L^2(\Omega)]^2},$$

and

$$\|(\boldsymbol{\sigma}, \mathbf{u}, \boldsymbol{\gamma}) - (\boldsymbol{\sigma}_h, \mathbf{u}_h, \boldsymbol{\gamma}_h)\|_{\mathbf{H}_0} \leq \tilde{C} \inf_{(\boldsymbol{\tau}_h, \mathbf{v}_h, \boldsymbol{\eta}_h) \in \mathbf{H}_{0,h}} \|(\boldsymbol{\sigma}, \mathbf{u}, \boldsymbol{\gamma}) - (\boldsymbol{\tau}_h, \mathbf{v}_h, \boldsymbol{\eta}_h)\|_{\mathbf{H}_0}. \tag{11}$$

Proof. It follows from Theorem 2.1, Lax-Milgram's Lemma, and Céa's estimate. □

It is important to emphasize here that the main advantage of the augmented approach (10), as compared with the traditional mixed finite element schemes for the linear elasticity problem (see *e.g.* [3]), is the possibility of choosing any finite element subspace $\mathbf{H}_{0,h}$ of $\mathbf{H}_0$.

On the other hand, an inmediate consequence of the definition of the continuous and discrete augmented formulations is the Galerkin orthogonality

$$A((\boldsymbol{\sigma} - \boldsymbol{\sigma}_h, \mathbf{u} - \mathbf{u}_h, \boldsymbol{\gamma} - \boldsymbol{\gamma}_h), (\boldsymbol{\tau}_h, \mathbf{v}_h, \boldsymbol{\eta}_h)) = 0 \qquad \forall (\boldsymbol{\tau}_h, \mathbf{v}_h, \boldsymbol{\eta}_h) \in \mathbf{H}_{0,h}. \tag{12}$$

Next, we recall the specific space $\mathbf{H}_{0,h}$ introduced in [10], which is the simplest finite element subspace of $\mathbf{H}_0$. To this end, we first let $\{\mathcal{T}_h\}_{h>0}$ be a regular family of triangulations of the polygonal region $\bar{\Omega}$ by triangles T of diameter h_T with mesh size $h := \max\{h_T : T \in \mathcal{T}_h\}$, and such that there holds $\bar{\Omega} = \cup\{T : T \in \mathcal{T}_h\}$. In addition, given an integer $\ell \geq 0$ and a subset S of $\mathbb{R}^2$, we denote by $\mathbb{P}_\ell(S)$ the space of polynomials in two variables defined in S of total degree at most ℓ, and for each $T \in \mathcal{T}_h$ we introduce the local Raviart-Thomas space of order zero (*cf.* [3,12]),

$$\mathbb{RT}_0(T) := \text{span}\left\{ \begin{pmatrix} 1 \\ 0 \end{pmatrix}, \begin{pmatrix} 0 \\ 1 \end{pmatrix}, \begin{pmatrix} x_1 \\ x_2 \end{pmatrix} \right\} \subseteq [\mathbb{P}_1(T)]^2,$$

where $\begin{pmatrix} x_1 \\ x_2 \end{pmatrix}$ is a generic vector of $\mathbb{R}^2$. Then, defining

$$H_h^{\boldsymbol{\sigma}} := \left\{ \boldsymbol{\tau}_h \in H(\mathbf{div}; \Omega): \quad \boldsymbol{\tau}_h|_T \in [\mathbb{RT}_0(T)^{\mathrm{t}}]^2 \qquad \forall T \in \mathcal{T}_h \right\}, \tag{13}$$

$$X_h := \left\{ v_h \in C(\bar{\Omega}): \quad v_h|_T \in \mathbb{P}_1(T) \quad \forall T \in \mathcal{T}_h \right\}, \tag{14}$$

and

$$H_h^{\mathbf{u}} := X_h \times X_h, \tag{15}$$

we take

$$\mathbf{H}_{0,h} := H_{0,h}^{\boldsymbol{\sigma}} \times H_{0,h}^{\mathbf{u}} \times H_h^{\boldsymbol{\gamma}}, \tag{16}$$

where

$$H_{0,h}^{\boldsymbol{\sigma}} := \left\{ \boldsymbol{\tau}_h \in H_h^{\boldsymbol{\sigma}} : \quad \int_{\Omega} \mathrm{tr}(\boldsymbol{\tau}_h) = 0 \right\}, \tag{17}$$

$$H_{0,h}^{\mathbf{u}} := \left\{ \mathbf{v}_h \in H_h^{\mathbf{u}} : \quad \mathbf{v}_h = \mathbf{0} \quad \text{on} \quad \Gamma \right\}, \tag{18}$$

and

$$H_h^{\boldsymbol{\gamma}} := \left\{ \boldsymbol{\eta}_h \in [L^2(\Omega)]_{\mathtt{skew}}^{2\times 2} : \quad \boldsymbol{\eta}_h|_T \in [\mathbb{P}_0(T)]^{2\times 2} \quad \forall T \in \mathcal{T}_h \right\}. \tag{19}$$

The following theorem provides the rate of convergence of (10) when the specific finite element subspace (16) is utilized.

Theorem 2.3. *Let $(\boldsymbol{\sigma}, \mathbf{u}, \boldsymbol{\gamma}) \in \mathbf{H}_0$ and $(\boldsymbol{\sigma}_h, \mathbf{u}_h, \boldsymbol{\gamma}_h) \in \mathbf{H}_{0,h} := H_{0,h}^{\boldsymbol{\sigma}} \times H_{0,h}^{\mathbf{u}} \times H_h^{\boldsymbol{\gamma}}$ be the unique solutions of the continuous and discrete augmented mixed formulations (4) and (10), respectively. Assume that $\boldsymbol{\sigma} \in [H^r(\Omega)]^{2\times 2}$, $\mathbf{div}(\boldsymbol{\sigma}) \in [H^r(\Omega)]^2$, $\mathbf{u} \in [H^{r+1}(\Omega)]^2$, and $\boldsymbol{\gamma} \in [H^r(\Omega)]^{2\times 2}$, for some $r \in (0,1]$. Then there exists $C > 0$, independent of h and λ, such that*

$$\|(\boldsymbol{\sigma}, \mathbf{u}, \boldsymbol{\gamma}) - (\boldsymbol{\sigma}_h, \mathbf{u}_h, \boldsymbol{\gamma}_h)\|_{\mathbf{H}_0} \leq C\,h^r \left\{ \|\boldsymbol{\sigma}\|_{[H^r(\Omega)]^{2\times 2}} + \|\mathbf{div}(\boldsymbol{\sigma})\|_{[H^r(\Omega)]^2} + \|\mathbf{u}\|_{[H^{r+1}(\Omega)]^2} + \|\boldsymbol{\gamma}\|_{[H^r(\Omega)]^{2\times 2}} \right\}.$$

Proof. It is a consequence of Céa's estimate, the approximation properties of the subspaces defining $\mathbf{H}_{0,h}$, and suitable interpolation theorems in the corresponding function spaces. See Section 4.1 in [10] for more details. $\square$

3. A residual based *a posteriori* error estimator

In this section we derive a residual based *a posteriori* error estimator for (10). First we introduce several notations. Given $T \in \mathcal{T}_h$, we let $E(T)$ be the set of its edges, and let E_h be the set of all edges of the triangulation $\mathcal{T}_h$. Then we write $E_h = E_h(\Omega) \cup E_h(\Gamma)$, where $E_h(\Omega) := \{e \in E_h : e \subseteq \Omega\}$ and $E_h(\Gamma) := \{e \in E_h : e \subseteq \Gamma\}$. In what follows, h_e stands for the length of edge $e \in E_h$. Further, given $\boldsymbol{\tau} \in [L^2(\Omega)]^{2\times 2}$ (such that $\boldsymbol{\tau}|_T \in C(T)$ on each $T \in \mathcal{T}_h$), an edge $e \in E(T) \cap E_h(\Omega)$, and the unit tangential vector $\mathbf{t}_T$ along e, we let $J[\boldsymbol{\tau} \mathbf{t}_T]$ be the corresponding jump across e, that is, $J[\boldsymbol{\tau} \mathbf{t}_T] := (\boldsymbol{\tau}|_T - \boldsymbol{\tau}|_{T'})|_e \mathbf{t}_T$, where T' is the other triangle of $\mathcal{T}_h$ having e as an edge. Abusing notation, when $e \in E_h(\Gamma)$, we also write $J[\boldsymbol{\tau} \mathbf{t}_T] := \boldsymbol{\tau}|_e \mathbf{t}_T$. We recall here that $\mathbf{t}_T := (-\nu_2, \nu_1)^{\mathtt{t}}$ where $\boldsymbol{\nu}_T := (\nu_1, \nu_2)^{\mathtt{t}}$ is the unit outward normal to ∂T. Analogously, we define the normal jumps $J[\boldsymbol{\tau} \boldsymbol{\nu}_T]$. In addition, given scalar, vector, and tensor valued fields v, $\boldsymbol{\varphi} := (\varphi_1, \varphi_2)$, and $\boldsymbol{\tau} := (\tau_{ij})$, respectively, we let

$$\mathbf{curl}(v) := \begin{pmatrix} -\frac{\partial v}{\partial x_2} \\ \frac{\partial v}{\partial x_1} \end{pmatrix}, \quad \underline{\mathbf{curl}}(\boldsymbol{\varphi}) := \begin{pmatrix} \mathbf{curl}(\varphi_1)^{\mathtt{t}} \\ \mathbf{curl}(\varphi_2)^{\mathtt{t}} \end{pmatrix}, \quad \text{and} \quad \mathrm{curl}(\boldsymbol{\tau}) := \begin{pmatrix} \frac{\partial \tau_{12}}{\partial x_1} - \frac{\partial \tau_{11}}{\partial x_2} \\ \frac{\partial \tau_{22}}{\partial x_1} - \frac{\partial \tau_{21}}{\partial x_2} \end{pmatrix}.$$

Then, for $(\boldsymbol{\sigma}, \mathbf{u}, \boldsymbol{\gamma}) \in \mathbf{H}_0$ and $(\boldsymbol{\sigma}_h, \mathbf{u}_h, \boldsymbol{\gamma}_h) \in \mathbf{H}_{0,h}$ being the solutions of the continuous and discrete formulations (4) and (10), respectively, we define an error indicator θ_T as follows:

$$
\begin{aligned}
\theta_T^2 \quad := \quad & \|\mathbf{f} + \mathbf{div}\,(\boldsymbol{\sigma}_h)\|_{[L^2(T)]^2}^2 \; + \; \|\boldsymbol{\sigma}_h - \boldsymbol{\sigma}_h^{\mathrm{t}}\|_{[L^2(T)]^{2\times 2}}^2 \; + \; \|\boldsymbol{\gamma}_h - \tfrac{1}{2}(\nabla \mathbf{u}_h - (\nabla \mathbf{u}_h)^{\mathrm{t}})\|_{[L^2(T)]^{2\times 2}}^2 \\[4pt]
& + \quad h_T^2 \left\{ \|\operatorname{curl}(\mathcal{C}^{-1}\boldsymbol{\sigma}_h + \boldsymbol{\gamma}_h)\|_{[L^2(T)]^2}^2 \; + \; \|\operatorname{curl}(\mathcal{C}^{-1}(\mathbf{e}(\mathbf{u}_h) - \mathcal{C}^{-1}\boldsymbol{\sigma}_h))\|_{[L^2(T)]^2}^2 \right\} \\[4pt]
& + \quad \sum_{e \in E(T)} h_e \left\{ \|J[(\mathcal{C}^{-1}\boldsymbol{\sigma}_h - \nabla \mathbf{u}_h + \boldsymbol{\gamma}_h)\mathbf{t}_T]\|_{[L^2(e)]^2}^2 \; + \; \|J[(\mathcal{C}^{-1}(\mathbf{e}(\mathbf{u}_h) - \mathcal{C}^{-1}\boldsymbol{\sigma}_h))\mathbf{t}_T]\|_{[L^2(e)]^2}^2 \right\} \\[4pt]
& + \quad h_T^2 \,\|\mathbf{div}\,(\mathbf{e}(\mathbf{u}_h) - \tfrac{1}{2}(\mathcal{C}^{-1}\boldsymbol{\sigma}_h + (\mathcal{C}^{-1}\boldsymbol{\sigma}_h)^{\mathrm{t}}))\|_{[L^2(T)]^2}^2 \\[4pt]
& + \quad h_T^2 \,\|\mathbf{div}\,(\boldsymbol{\gamma}_h - \tfrac{1}{2}(\nabla \mathbf{u}_h - (\nabla \mathbf{u}_h)^{\mathrm{t}}))\|_{[L^2(T)]^2}^2 \\[4pt]
& + \quad \sum_{e \in E(T) \cap E_h(\Omega)} h_e \,\|J[(\mathbf{e}(\mathbf{u}_h) - \tfrac{1}{2}(\mathcal{C}^{-1}\boldsymbol{\sigma}_h + (\mathcal{C}^{-1}\boldsymbol{\sigma}_h)^{\mathrm{t}}))\boldsymbol{\nu}_T]\|_{[L^2(e)]^2}^2 \\[4pt]
& + \quad \sum_{e \in E(T) \cap E_h(\Omega)} h_e \,\|J[(\boldsymbol{\gamma}_h - \tfrac{1}{2}(\nabla \mathbf{u}_h - (\nabla \mathbf{u}_h)^{\mathrm{t}}))\boldsymbol{\nu}_T]\|_{[L^2(e)]^2}^2 \,.
\end{aligned}
\tag{20}
$$

The residual character of each term on the right-hand side of (20) is quite clear. In addition, we observe that some of these terms are known from residual estimators for the non-augmented mixed finite element method in linear elasticity (see *e.g.* [5]), but most of them are new since, as we show below, they arise from the new Galerkin least-squares terms introduced in the augmented formulation. We also mention that, as usual, the expression $\boldsymbol{\theta} := \left\{ \sum_{T \in \mathcal{T}_h} \theta_T^2 \right\}^{1/2}$ is employed as the global residual error estimator.

The following theorem is the main result of this paper.

Theorem 3.1. *Let $(\boldsymbol{\sigma}, \mathbf{u}, \boldsymbol{\gamma}) \in \mathbf{H}_0$ and $(\boldsymbol{\sigma}_h, \mathbf{u}_h, \boldsymbol{\gamma}_h) \in \mathbf{H}_{0,h}$ be the unique solutions of (4) and (10), respectively. Then there exist $C_{\mathtt{eff}}, C_{\mathtt{rel}} > 0$, independent of h and λ, such that*

$$
C_{\mathtt{eff}}\,\boldsymbol{\theta} \; \leq \; \|(\boldsymbol{\sigma} - \boldsymbol{\sigma}_h, \mathbf{u} - \mathbf{u}_h, \boldsymbol{\gamma} - \boldsymbol{\gamma}_h)\|_{\mathbf{H}_0} \; \leq \; C_{\mathtt{rel}}\,\boldsymbol{\theta}\,.
\tag{21}
$$

The so-called efficiency (lower bound in (21)) is proved below in Section 4 and the reliability estimate (upper bound in (21)) is derived throughout the rest of the present section. The method that we use to prove reliability combines a procedure employed in mixed finite element schemes (see *e.g.* [4,5]), where an auxiliary problem needs to be defined, with the integration by parts and Clément interpolant technique usually applied to primal finite element methods (see [13]). We emphasize that just one of these approaches by itself would not suffice.

We begin with the following preliminary estimate.

Lemma 3.1. *There exists $C > 0$, independent of h and λ, such that*

$$
\begin{aligned}
& C \, \|(\boldsymbol{\sigma} - \boldsymbol{\sigma}_h, \mathbf{u} - \mathbf{u}_h, \boldsymbol{\gamma} - \boldsymbol{\gamma}_h)\|_{\mathbf{H}_0} \\
& \leq \sup_{\substack{\mathbf{0} \neq (\boldsymbol{\tau}, \mathbf{v}, \boldsymbol{\eta}) \in \mathbf{H}_0 \\ \mathbf{div}\,(\boldsymbol{\tau}) = \mathbf{0}}} \frac{A((\boldsymbol{\sigma} - \boldsymbol{\sigma}_h, \mathbf{u} - \mathbf{u}_h, \boldsymbol{\gamma} - \boldsymbol{\gamma}_h), (\boldsymbol{\tau}, \mathbf{v}, \boldsymbol{\eta}))}{\|(\boldsymbol{\tau}, \mathbf{v}, \boldsymbol{\eta})\|_{\mathbf{H}_0}} \; + \; \|\mathbf{f} + \mathbf{div}\,(\boldsymbol{\sigma}_h)\|_{[L^2(\Omega)]^2}\,.
\end{aligned}
\tag{22}
$$

Proof. Let us define $\boldsymbol{\sigma}^* = \mathbf{e}(\mathbf{z})$, where $\mathbf{z} \in [H_0^1(\Omega)]^2$ is the unique solution of the boundary value problem: $-\mathbf{div}\,(\mathbf{e}(\mathbf{z})) = \mathbf{f} + \mathbf{div}\,(\boldsymbol{\sigma}_h)$ in Ω, $\mathbf{z} = \mathbf{0}$ on Γ. It follows that $\boldsymbol{\sigma}^* \in H_0$, and the corresponding continuous dependence result establishes the existence of $c > 0$ such that

$$
\|\boldsymbol{\sigma}^*\|_{H(\mathbf{div}\,;\Omega)} \; \leq \; c\,\|\mathbf{f} + \mathbf{div}\,(\boldsymbol{\sigma}_h)\|_{[L^2(\Omega)]^2}\,.
\tag{23}
$$

In addition, it is easy to see that $\mathbf{div}\,(\boldsymbol{\sigma} - \boldsymbol{\sigma}_h - \boldsymbol{\sigma}^*) = \mathbf{0}$ in Ω. Then, using the coercivity of A (*cf.* (8)), we find that

$$\alpha \, \|(\boldsymbol{\sigma} - \boldsymbol{\sigma}_h - \boldsymbol{\sigma}^*, \mathbf{u} - \mathbf{u}_h, \boldsymbol{\gamma} - \boldsymbol{\gamma}_h)\|_{\mathbf{H}_0}^2$$
$$\leq A((\boldsymbol{\sigma} - \boldsymbol{\sigma}_h - \boldsymbol{\sigma}^*, \mathbf{u} - \mathbf{u}_h, \boldsymbol{\gamma} - \boldsymbol{\gamma}_h), (\boldsymbol{\sigma} - \boldsymbol{\sigma}_h - \boldsymbol{\sigma}^*, \mathbf{u} - \mathbf{u}_h, \boldsymbol{\gamma} - \boldsymbol{\gamma}_h))$$
$$= A((\boldsymbol{\sigma} - \boldsymbol{\sigma}_h, \mathbf{u} - \mathbf{u}_h, \boldsymbol{\gamma} - \boldsymbol{\gamma}_h), (\boldsymbol{\sigma} - \boldsymbol{\sigma}_h - \boldsymbol{\sigma}^*, \mathbf{u} - \mathbf{u}_h, \boldsymbol{\gamma} - \boldsymbol{\gamma}_h))$$
$$- A((\boldsymbol{\sigma}^*, \mathbf{0}, \mathbf{0}), (\boldsymbol{\sigma} - \boldsymbol{\sigma}_h - \boldsymbol{\sigma}^*, \mathbf{u} - \mathbf{u}_h, \boldsymbol{\gamma} - \boldsymbol{\gamma}_h)),$$

which, employing the boundedness of A (*cf.* (7)), yields

$$\alpha \, \|(\boldsymbol{\sigma} - \boldsymbol{\sigma}_h - \boldsymbol{\sigma}^*, \mathbf{u} - \mathbf{u}_h, \boldsymbol{\gamma} - \boldsymbol{\gamma}_h)\|_{\mathbf{H}_0}$$
$$\leq \sup_{\substack{\mathbf{0} \neq (\boldsymbol{\tau}, \mathbf{v}, \boldsymbol{\eta}) \in \mathbf{H}_0 \\ \mathbf{div}\,(\boldsymbol{\tau}) = \mathbf{0}}} \frac{A((\boldsymbol{\sigma} - \boldsymbol{\sigma}_h, \mathbf{u} - \mathbf{u}_h, \boldsymbol{\gamma} - \boldsymbol{\gamma}_h), (\boldsymbol{\tau}, \mathbf{v}, \boldsymbol{\eta}))}{\|(\boldsymbol{\tau}, \mathbf{v}, \boldsymbol{\eta})\|_{\mathbf{H}_0}} \;+\; M \, \|\boldsymbol{\sigma}^*\|_{H(\mathbf{div}\,;\Omega)} \,. \quad (24)$$

Hence, (22) follows straightforwardly from the triangle inequality, (23), and (24). $\qquad\square$

It remains to bound the first term on the right-hand side of (22). To this end, we will make use of the well known Clément interpolation operator $I_h : H^1(\Omega) \to X_h$ (*cf.* [7]), with X_h given by (14), which satisfies the standard local approximation properties stated below in Lemma 3.2. It is important to remark that I_h is defined in [7] so that $I_h(v) \in X_h \cap H_0^1(\Omega)$ for all $v \in H_0^1(\Omega)$.

Lemma 3.2. *There exist constants c_1, $c_2 > 0$, independent of h, such that for all $v \in H^1(\Omega)$ there holds*

$$\|v - I_h(v)\|_{L^2(T)} \leq c_1 \, h_T \, \|v\|_{H^1(\Delta(T))} \quad \forall T \in \mathcal{T}_h \,,$$

and

$$\|v - I_h(v)\|_{L^2(e)} \leq c_2 \, h_e^{1/2} \, \|v\|_{H^1(\Delta(e))} \quad \forall e \in E_h \,,$$

where $\Delta(T) := \cup\{T' \in \mathcal{T}_h : \quad T' \cap T \neq \emptyset\}$, and $\Delta(e) := \cup\{T' \in \mathcal{T}_h : \quad T' \cap e \neq \emptyset\}$.

Proof. See [7]. $\qquad\square$

We now let $(\boldsymbol{\tau}, \mathbf{v}, \boldsymbol{\eta}) \in \mathbf{H}_0$, $(\boldsymbol{\tau}, \mathbf{v}, \boldsymbol{\eta}) \neq \mathbf{0}$, be such that $\mathbf{div}\,(\boldsymbol{\tau}) = \mathbf{0}$ in Ω. Since Ω is connected, there exists a stream function $\boldsymbol{\varphi} := (\varphi_1, \varphi_2) \in [H^1(\Omega)]^2$ such that $\int_\Omega \varphi_1 = \int_\Omega \varphi_2 = 0$ and $\boldsymbol{\tau} = \underline{\mathbf{curl}}(\boldsymbol{\varphi})$. Then, denoting $\boldsymbol{\varphi}_h := (\varphi_{1,h}, \varphi_{2,h})$, with $\varphi_{i,h} := I_h(\varphi_i)$, $i \in \{1,2\}$, the Clément interpolant of φ_i, we define $\boldsymbol{\tau}_h := \underline{\mathbf{curl}}(\boldsymbol{\varphi}_h)$. Note that there holds the decomposition $\boldsymbol{\tau}_h = \boldsymbol{\tau}_{h,0} + d_h\,\mathbf{I}$, where $\boldsymbol{\tau}_{h,0} \in H_{0,h}^{\boldsymbol{\sigma}}$ and $d_h = \frac{\int_\Omega tr(\boldsymbol{\tau}_h)}{2|\Omega|} \in \mathbb{R}$. From the orthogonality relation (12) it follows that

$$A((\boldsymbol{\sigma} - \boldsymbol{\sigma}_h, \mathbf{u} - \mathbf{u}_h, \boldsymbol{\gamma} - \boldsymbol{\gamma}_h), (\boldsymbol{\tau}, \mathbf{v}, \boldsymbol{\eta})) = A((\boldsymbol{\sigma} - \boldsymbol{\sigma}_h, \mathbf{u} - \mathbf{u}_h, \boldsymbol{\gamma} - \boldsymbol{\gamma}_h), (\boldsymbol{\tau} - \boldsymbol{\tau}_{h,0}, \mathbf{v} - \mathbf{v}_h, \boldsymbol{\eta})), \qquad (25)$$

where $\mathbf{v}_h := (I_h(v_1), I_h(v_2)) \in H_{0,h}^{\mathbf{u}}$ is the vector Clément interpolant of $\mathbf{v} := (v_1, v_2) \in [H_0^1(\Omega)]^2$. Since $\int_\Omega \mathrm{tr}(\boldsymbol{\sigma} - \boldsymbol{\sigma}_h) = 0$ and $\mathbf{u} - \mathbf{u}_h = \mathbf{0}$ on Γ, we deduce, using the orthogonality between symmetric and skew-symmetric tensors, that

$$A((\boldsymbol{\sigma} - \boldsymbol{\sigma}_h, \mathbf{u} - \mathbf{u}_h, \boldsymbol{\gamma} - \boldsymbol{\gamma}_h), (d_h\mathbf{I}, \mathbf{0}, \mathbf{0})) = 0 \,.$$

Hence, (25) and (4) give

$$A((\boldsymbol{\sigma} - \boldsymbol{\sigma}_h, \mathbf{u} - \mathbf{u}_h, \boldsymbol{\gamma} - \boldsymbol{\gamma}_h), (\boldsymbol{\tau}, \mathbf{v}, \boldsymbol{\eta})) = A((\boldsymbol{\sigma} - \boldsymbol{\sigma}_h, \mathbf{u} - \mathbf{u}_h, \boldsymbol{\gamma} - \boldsymbol{\gamma}_h), (\boldsymbol{\tau} - \boldsymbol{\tau}_h, \mathbf{v} - \mathbf{v}_h, \boldsymbol{\eta}))$$
$$= F(\boldsymbol{\tau} - \boldsymbol{\tau}_h, \mathbf{v} - \mathbf{v}_h, \boldsymbol{\eta}) - A((\boldsymbol{\sigma}_h, \mathbf{u}_h, \boldsymbol{\gamma}_h), (\boldsymbol{\tau} - \boldsymbol{\tau}_h, \mathbf{v} - \mathbf{v}_h, \boldsymbol{\eta})) \,.$$

According to the definitions of the forms A and F (*cf.* (5), (6)), noting that $\mathbf{div}\,(\boldsymbol{\tau}-\boldsymbol{\tau}_h) = \mathbf{div}\,\underline{\mathbf{curl}}(\boldsymbol{\varphi}-\boldsymbol{\varphi}_h) = \mathbf{0}$, and using again the above mentioned orthogonality, we find, after some algebraic manipulations, that

$$
\begin{aligned}
A((\boldsymbol{\sigma}-\boldsymbol{\sigma}_h,\mathbf{u}-\mathbf{u}_h,\boldsymbol{\gamma}-\boldsymbol{\gamma}_h),(\boldsymbol{\tau},\mathbf{v},\boldsymbol{\eta})) &= \int_\Omega (\mathbf{f}+\mathbf{div}\,(\boldsymbol{\sigma}_h))\cdot(\mathbf{v}-\mathbf{v}_h) \\
&+ \int_\Omega \left\{ \frac{1}{2}(\boldsymbol{\sigma}_h-\boldsymbol{\sigma}_h^{\mathsf{t}}) - \kappa_3\left(\boldsymbol{\gamma}_h-\frac{1}{2}(\nabla\mathbf{u}_h-(\nabla\mathbf{u}_h)^{\mathsf{t}})\right)\right\}:\boldsymbol{\eta} \\
&- \int_\Omega \left\{ (\mathcal{C}^{-1}\boldsymbol{\sigma}_h-\nabla\mathbf{u}_h+\boldsymbol{\gamma}_h)+\kappa_1\,\mathcal{C}^{-1}(\mathbf{e}(\mathbf{u}_h)-\mathcal{C}^{-1}\boldsymbol{\sigma}_h)\right\}:(\boldsymbol{\tau}-\boldsymbol{\tau}_h) \\
- \int_\Omega \Big\{ \kappa_1\left(\mathbf{e}(\mathbf{u}_h)-\frac{1}{2}(\mathcal{C}^{-1}\boldsymbol{\sigma}_h+(\mathcal{C}^{-1}\boldsymbol{\sigma}_h)^{\mathsf{t}})\right)&+\kappa_3\left(\boldsymbol{\gamma}_h-\frac{1}{2}(\nabla\mathbf{u}_h-(\nabla\mathbf{u}_h)^{\mathsf{t}})\right)\Big\}:\nabla(\mathbf{v}-\mathbf{v}_h).
\end{aligned}
\tag{26}
$$

The rest of the proof of reliability consists in deriving suitable upper bounds for each of the terms appearing on the right-hand side of (26). We begin by noticing that direct applications of the Cauchy-Schwarz inequality give

$$
\left|\int_\Omega \frac{1}{2}(\boldsymbol{\sigma}_h-\boldsymbol{\sigma}_h^{\mathsf{t}}):\boldsymbol{\eta}\right| \le \|\boldsymbol{\sigma}_h-\boldsymbol{\sigma}_h^{\mathsf{t}}\|_{[L^2(\Omega)]^{2\times2}}\ \|\boldsymbol{\eta}\|_{[L^2(\Omega)]^{2\times2}}\,,
\tag{27}
$$

and

$$
\left|\int_\Omega (\boldsymbol{\gamma}_h-\frac{1}{2}(\nabla\mathbf{u}_h-(\nabla\mathbf{u}_h)^{\mathsf{t}})):\boldsymbol{\eta}\right| \le \left\|\boldsymbol{\gamma}_h-\frac{1}{2}(\nabla\mathbf{u}_h-(\nabla\mathbf{u}_h)^{\mathsf{t}})\right\|_{[L^2(\Omega)]^{2\times2}}\ \|\boldsymbol{\eta}\|_{[L^2(\Omega)]^{2\times2}}\,.
\tag{28}
$$

The decomposition $\Omega = \cup_{T\in\mathcal{T}_h}T$ and the integration by parts formula on each element are employed next to handle the terms from the third and fourth rows of (26). We first replace $(\boldsymbol{\tau}-\boldsymbol{\tau}_h)$ by $\underline{\mathbf{curl}}(\boldsymbol{\varphi}-\boldsymbol{\varphi}_h)$ and use that $\mathrm{curl}(\nabla\mathbf{u}_h) = \mathbf{0}$ in each triangle $T\in\mathcal{T}_h$, to obtain

$$
\begin{aligned}
\int_\Omega (\mathcal{C}^{-1}\boldsymbol{\sigma}_h-\nabla\mathbf{u}_h+\boldsymbol{\gamma}_h):(\boldsymbol{\tau}-\boldsymbol{\tau}_h) &= \sum_{T\in\mathcal{T}_h}\int_T (\mathcal{C}^{-1}\boldsymbol{\sigma}_h-\nabla\mathbf{u}_h+\boldsymbol{\gamma}_h):\underline{\mathbf{curl}}(\boldsymbol{\varphi}-\boldsymbol{\varphi}_h) \\
&= \sum_{T\in\mathcal{T}_h}\int_T \mathrm{curl}(\mathcal{C}^{-1}\boldsymbol{\sigma}_h+\boldsymbol{\gamma}_h)\cdot(\boldsymbol{\varphi}-\boldsymbol{\varphi}_h) \\
&\quad - \sum_{e\in E_h}\langle J[(\mathcal{C}^{-1}\boldsymbol{\sigma}_h-\nabla\mathbf{u}_h+\boldsymbol{\gamma}_h)\mathbf{t}_T],\boldsymbol{\varphi}-\boldsymbol{\varphi}_h\rangle_{[L^2(e)]^2}\,,
\end{aligned}
\tag{29}
$$

and

$$
\begin{aligned}
\int_\Omega \mathcal{C}^{-1}(\mathbf{e}(\mathbf{u}_h)-\mathcal{C}^{-1}\boldsymbol{\sigma}_h):(\boldsymbol{\tau}-\boldsymbol{\tau}_h) &= \sum_{T\in\mathcal{T}_h}\int_T \mathcal{C}^{-1}(\mathbf{e}(\mathbf{u}_h)-\mathcal{C}^{-1}\boldsymbol{\sigma}_h):\underline{\mathbf{curl}}(\boldsymbol{\varphi}-\boldsymbol{\varphi}_h) \\
&= \sum_{T\in\mathcal{T}_h}\int_T \mathrm{curl}(\mathcal{C}^{-1}(\mathbf{e}(\mathbf{u}_h)-\mathcal{C}^{-1}\boldsymbol{\sigma}_h))\cdot(\boldsymbol{\varphi}-\boldsymbol{\varphi}_h) \\
&\quad - \sum_{e\in E_h}\langle J[(\mathcal{C}^{-1}(\mathbf{e}(\mathbf{u}_h)-\mathcal{C}^{-1}\boldsymbol{\sigma}_h))\mathbf{t}_T],\boldsymbol{\varphi}-\boldsymbol{\varphi}_h\rangle_{[L^2(e)]^2}\,.
\end{aligned}
\tag{30}
$$

On the other hand, using that $\mathbf{v} - \mathbf{v}_h = \mathbf{0}$ on Γ, we easily get

$$\int_\Omega (\mathbf{e}(\mathbf{u}_h) - \frac{1}{2}(\mathcal{C}^{-1}\boldsymbol{\sigma}_h + (\mathcal{C}^{-1}\boldsymbol{\sigma}_h)^{\mathrm{t}})) : \nabla(\mathbf{v} - \mathbf{v}_h)$$
$$= -\sum_{T\in\mathcal{T}_h} \int_T \mathbf{div}\,(\mathbf{e}(\mathbf{u}_h) - \frac{1}{2}(\mathcal{C}^{-1}\boldsymbol{\sigma}_h + (\mathcal{C}^{-1}\boldsymbol{\sigma}_h)^{\mathrm{t}})) \cdot (\mathbf{v} - \mathbf{v}_h)$$
$$+ \sum_{e\in E_h(\Omega)} \langle J[(\mathbf{e}(\mathbf{u}_h) - \frac{1}{2}(\mathcal{C}^{-1}\boldsymbol{\sigma}_h + (\mathcal{C}^{-1}\boldsymbol{\sigma}_h)^{\mathrm{t}}))\boldsymbol{\nu}_T], \mathbf{v} - \mathbf{v}_h \rangle_{[L^2(e)]^2}, \quad (31)$$

and

$$\int_\Omega (\boldsymbol{\gamma}_h - \frac{1}{2}(\nabla\mathbf{u}_h - (\nabla\mathbf{u}_h)^{\mathrm{t}})) : \nabla(\mathbf{v} - \mathbf{v}_h)$$
$$= -\sum_{T\in\mathcal{T}_h} \int_T \mathbf{div}\,(\boldsymbol{\gamma}_h - \frac{1}{2}(\nabla\mathbf{u}_h - (\nabla\mathbf{u}_h)^{\mathrm{t}})) \cdot (\mathbf{v} - \mathbf{v}_h)$$
$$+ \sum_{e\in E_h(\Omega)} \langle J[(\boldsymbol{\gamma}_h - \frac{1}{2}(\nabla\mathbf{u}_h - (\nabla\mathbf{u}_h)^{\mathrm{t}}))\boldsymbol{\nu}_T], \mathbf{v} - \mathbf{v}_h \rangle_{[L^2(e)]^2}. \quad (32)$$

In what follows, we apply again the Cauchy-Schwarz inequality, Lemma 3.2, and the fact that the numbers of triangles in $\Delta(T)$ and $\Delta(e)$ are bounded, independently of h, to derive the estimates for the expression $\int_\Omega (\mathbf{f} + \mathbf{div}\,\boldsymbol{\sigma}_h) \cdot (\mathbf{v} - \mathbf{v}_h)$ in (26) and the right-hand sides of (29), (30), (31), and (32), with constants C independent of h and λ. Indeed, we easily have

$$\left| \int_\Omega (\mathbf{f} + \mathbf{div}\,\boldsymbol{\sigma}_h) \cdot (\mathbf{v} - \mathbf{v}_h) \right| \le \sum_{T\in\mathcal{T}_h} \|\mathbf{f} + \mathbf{div}\,\boldsymbol{\sigma}_h\|_{[L^2(T)]^2} \|\mathbf{v} - \mathbf{v}_h\|_{[L^2(T)]^2}$$
$$\le c_1 \sum_{T\in\mathcal{T}_h} \|\mathbf{f} + \mathbf{div}\,\boldsymbol{\sigma}_h\|_{[L^2(T)]^2}\, h_T\, \|\mathbf{v}\|_{[H^1(\Delta(T)]^2}$$
$$\le C \left\{ \sum_{T\in\mathcal{T}_h} h_T^2 \|\mathbf{f} + \mathbf{div}\,\boldsymbol{\sigma}_h\|_{[L^2(T)]^2}^2 \right\}^{1/2} \|\mathbf{v}\|_{[H^1(\Omega)]^2}. \quad (33)$$

In addition, for the terms containing the stream function $\boldsymbol{\varphi}$ (cf. (29), (30)), we get

$$\left| \sum_{T\in\mathcal{T}_h} \int_T \mathrm{curl}(\mathcal{C}^{-1}\boldsymbol{\sigma}_h + \boldsymbol{\gamma}_h) \cdot (\boldsymbol{\varphi} - \boldsymbol{\varphi}_h) \right| \le \sum_{T\in\mathcal{T}_h} \|\mathrm{curl}(\mathcal{C}^{-1}\boldsymbol{\sigma}_h + \boldsymbol{\gamma}_h)\|_{[L^2(T)]^2} \|\boldsymbol{\varphi} - \boldsymbol{\varphi}_h\|_{[L^2(T)]^2}$$
$$\le c_1 \sum_{T\in\mathcal{T}_h} \|\mathrm{curl}(\mathcal{C}^{-1}\boldsymbol{\sigma}_h + \boldsymbol{\gamma}_h)\|_{[L^2(T)]^2}\, h_T\, \|\boldsymbol{\varphi}\|_{[H^1(\Delta(T)]^2}$$
$$\le C \left\{ \sum_{T\in\mathcal{T}_h} h_T^2 \|\mathrm{curl}(\mathcal{C}^{-1}\boldsymbol{\sigma}_h + \boldsymbol{\gamma}_h)\|_{[L^2(T)]^2}^2 \right\}^{1/2} \|\boldsymbol{\varphi}\|_{[H^1(\Omega)]^2}, \quad (34)$$

$$\left| \sum_{T \in \mathcal{T}_h} \int_T \text{curl}(\mathcal{C}^{-1}(\mathbf{e}(\mathbf{u}_h) - \mathcal{C}^{-1}\boldsymbol{\sigma}_h)) \cdot (\boldsymbol{\varphi} - \boldsymbol{\varphi}_h) \right|$$

$$\leq \sum_{T \in \mathcal{T}_h} \| \text{curl}(\mathcal{C}^{-1}(\mathbf{e}(\mathbf{u}_h) - \mathcal{C}^{-1}\boldsymbol{\sigma}_h)) \|_{[L^2(T)]^2} \| \boldsymbol{\varphi} - \boldsymbol{\varphi}_h \|_{[L^2(T)]^2}$$

$$\leq c_1 \sum_{T \in \mathcal{T}_h} \| \text{curl}(\mathcal{C}^{-1}(\mathbf{e}(\mathbf{u}_h) - \mathcal{C}^{-1}\boldsymbol{\sigma}_h)) \|_{[L^2(T)]^2} \, h_T \, \| \boldsymbol{\varphi} \|_{[H^1(\Delta(T))]^2}$$

$$\leq C \left\{ \sum_{T \in \mathcal{T}_h} h_T^2 \, \| \text{curl}(\mathcal{C}^{-1}(\mathbf{e}(\mathbf{u}_h) - \mathcal{C}^{-1}\boldsymbol{\sigma}_h)) \|_{[L^2(T)]^2}^2 \right\}^{1/2} \| \boldsymbol{\varphi} \|_{[H^1(\Omega)]^2} , \tag{35}$$

$$\left| \sum_{e \in E_h} \langle J[(\mathcal{C}^{-1}\boldsymbol{\sigma}_h - \nabla \mathbf{u}_h + \boldsymbol{\gamma}_h)\mathbf{t}_T], \boldsymbol{\varphi} - \boldsymbol{\varphi}_h \rangle_{[L^2(e)]^2} \right|$$

$$\leq \sum_{e \in E_h} \| J[(\mathcal{C}^{-1}\boldsymbol{\sigma}_h - \nabla \mathbf{u}_h + \boldsymbol{\gamma}_h)\mathbf{t}_T] \|_{[L^2(e)]^2} \| \boldsymbol{\varphi} - \boldsymbol{\varphi}_h \|_{[L^2(e)]^2}$$

$$\leq c_2 \sum_{e \in E_h} \| J[(\mathcal{C}^{-1}\boldsymbol{\sigma}_h - \nabla \mathbf{u}_h + \boldsymbol{\gamma}_h)\mathbf{t}_T] \|_{[L^2(e)]^2} \, h_e^{1/2} \, \| \boldsymbol{\varphi} \|_{[H^1(\Delta(e))]^2}$$

$$\leq C \left\{ \sum_{e \in E_h} h_e \, \| J[(\mathcal{C}^{-1}\boldsymbol{\sigma}_h - \nabla \mathbf{u}_h + \boldsymbol{\gamma}_h)\mathbf{t}_T] \|_{[L^2(e)]^2}^2 \right\}^{1/2} \| \boldsymbol{\varphi} \|_{[H^1(\Omega)]^2} , \tag{36}$$

and

$$\left| \sum_{e \in E_h} \langle J[(\mathcal{C}^{-1}(\mathbf{e}(\mathbf{u}_h) - \mathcal{C}^{-1}\boldsymbol{\sigma}_h))\mathbf{t}_T], \boldsymbol{\varphi} - \boldsymbol{\varphi}_h \rangle_{[L^2(e)]^2} \right|$$

$$\leq \sum_{e \in E_h} \| J[(\mathcal{C}^{-1}(\mathbf{e}(\mathbf{u}_h) - \mathcal{C}^{-1}\boldsymbol{\sigma}_h))\mathbf{t}_T] \|_{[L^2(e)]^2} \| \boldsymbol{\varphi} - \boldsymbol{\varphi}_h \|_{[L^2(e)]^2}$$

$$\leq c_2 \sum_{e \in E_h} \| J[(\mathcal{C}^{-1}(\mathbf{e}(\mathbf{u}_h) - \mathcal{C}^{-1}\boldsymbol{\sigma}_h))\mathbf{t}_T] \|_{[L^2(e)]^2} \, h_e^{1/2} \, \| \boldsymbol{\varphi} \|_{[H^1(\Delta(e))]^2}$$

$$\leq C \left\{ \sum_{e \in E_h} h_e \, \| J[(\mathcal{C}^{-1}(\mathbf{e}(\mathbf{u}_h) - \mathcal{C}^{-1}\boldsymbol{\sigma}_h))\mathbf{t}_T] \|_{[L^2(e)]^2}^2 \right\}^{1/2} \| \boldsymbol{\varphi} \|_{[H^1(\Omega)]^2} . \tag{37}$$

We observe here, thanks to the equivalence between $\| \boldsymbol{\varphi} \|_{[H^1(\Omega)]^2}$ and $| \boldsymbol{\varphi} |_{[H^1(\Omega)]^2}$, that

$$\| \boldsymbol{\varphi} \|_{[H^1(\Omega)]^2} \leq C \, | \boldsymbol{\varphi} |_{[H^1(\Omega)]^2} = C \, \| \underline{\mathbf{curl}}(\boldsymbol{\varphi}) \|_{[L^2(\Omega)]^2} = C \, \| \boldsymbol{\tau} \|_{H(\mathbf{div};\Omega)} , \tag{38}$$

which allows to replace $\| \boldsymbol{\varphi} \|_{[H^1(\Omega)]^2}$ by $\| \boldsymbol{\tau} \|_{H(\mathbf{div};\Omega)}$ in the above estimates (34)–(37).

Similarly, for the terms on the right-hand side of (31) and (32), we find that

$$
\left| \sum_{T \in \mathcal{T}_h} \int_T \mathbf{div}\,(\mathbf{e}(\mathbf{u}_h) - \frac{1}{2}(\mathcal{C}^{-1}\boldsymbol{\sigma}_h + (\mathcal{C}^{-1}\boldsymbol{\sigma}_h)^{\mathrm{t}})) \cdot (\mathbf{v} - \mathbf{v}_h) \right|
$$

$$
\leq \sum_{T \in \mathcal{T}_h} \| \mathbf{div}\,(\mathbf{e}(\mathbf{u}_h) - \frac{1}{2}(\mathcal{C}^{-1}\boldsymbol{\sigma}_h + (\mathcal{C}^{-1}\boldsymbol{\sigma}_h)^{\mathrm{t}}))\|_{[L^2(T)]^2} \,\|\mathbf{v} - \mathbf{v}_h\|_{[L^2(T)]^2}
$$

$$
\leq c_1 \sum_{T \in \mathcal{T}_h} \| \mathbf{div}\,(\mathbf{e}(\mathbf{u}_h) - \frac{1}{2}(\mathcal{C}^{-1}\boldsymbol{\sigma}_h + (\mathcal{C}^{-1}\boldsymbol{\sigma}_h)^{\mathrm{t}}))\|_{[L^2(T)]^2} \, h_T \,\|\mathbf{v}\|_{[H^1(\Delta(T)]^2}
$$

$$
\leq C \left\{ \sum_{T \in \mathcal{T}_h} h_T^2 \| \mathbf{div}\,(\mathbf{e}(\mathbf{u}_h) - \frac{1}{2}(\mathcal{C}^{-1}\boldsymbol{\sigma}_h + (\mathcal{C}^{-1}\boldsymbol{\sigma}_h)^{\mathrm{t}}))\|_{[L^2(T)]^2}^2 \right\}^{1/2} \,\|\mathbf{v}\|_{[H^1(\Omega)]^2}, \qquad (39)
$$

$$
\left| \sum_{T \in \mathcal{T}_h} \int_T \mathbf{div}\,(\boldsymbol{\gamma}_h - \frac{1}{2}(\nabla \mathbf{u}_h - (\nabla \mathbf{u}_h)^{\mathrm{t}})) \cdot (\mathbf{v} - \mathbf{v}_h) \right|
$$

$$
\leq \sum_{T \in \mathcal{T}_h} \| \mathbf{div}\,(\boldsymbol{\gamma}_h - \frac{1}{2}(\nabla \mathbf{u}_h - (\nabla \mathbf{u}_h)^{\mathrm{t}}))\|_{[L^2(T)]^2} \,\|\mathbf{v} - \mathbf{v}_h\|_{[L^2(T)]^2}
$$

$$
\leq c_1 \sum_{T \in \mathcal{T}_h} \| \mathbf{div}\,(\boldsymbol{\gamma}_h - \frac{1}{2}(\nabla \mathbf{u}_h - (\nabla \mathbf{u}_h)^{\mathrm{t}}))\|_{[L^2(T)]^2} \, h_T \,\|\mathbf{v}\|_{[H^1(\Delta(T)]^2}
$$

$$
\leq C \left\{ \sum_{T \in \mathcal{T}_h} h_T^2 \| \mathbf{div}\,(\boldsymbol{\gamma}_h - \frac{1}{2}(\nabla \mathbf{u}_h - (\nabla \mathbf{u}_h)^{\mathrm{t}}))\|_{[L^2(T)]^2}^2 \right\}^{1/2} \,\|\mathbf{v}\|_{[H^1(\Omega)]^2}, \qquad (40)
$$

$$
\left| \sum_{e \in E_h(\Omega)} \langle J[(\mathbf{e}(\mathbf{u}_h) - \frac{1}{2}(\mathcal{C}^{-1}\boldsymbol{\sigma}_h + (\mathcal{C}^{-1}\boldsymbol{\sigma}_h)^{\mathrm{t}}))\boldsymbol{\nu}_T], \mathbf{v} - \mathbf{v}_h \rangle_{[L^2(e)]^2} \right|
$$

$$
\leq \sum_{e \in E_h(\Omega)} \|J[(\mathbf{e}(\mathbf{u}_h) - \frac{1}{2}(\mathcal{C}^{-1}\boldsymbol{\sigma}_h + (\mathcal{C}^{-1}\boldsymbol{\sigma}_h)^{\mathrm{t}}))\boldsymbol{\nu}_T]\|_{[L^2(e)]^2} \,\|\mathbf{v} - \mathbf{v}_h\|_{[L^2(e)]^2}
$$

$$
\leq c_2 \sum_{e \in E_h(\Omega)} \|J[(\mathbf{e}(\mathbf{u}_h) - \frac{1}{2}(\mathcal{C}^{-1}\boldsymbol{\sigma}_h + (\mathcal{C}^{-1}\boldsymbol{\sigma}_h)^{\mathrm{t}}))\boldsymbol{\nu}_T]\|_{[L^2(e)]^2} \, h_e^{1/2} \,\|\mathbf{v}\|_{[H^1(\Delta(e))]^2}
$$

$$
\leq C \left\{ \sum_{e \in E_h(\Omega)} h_e \|J[(\mathbf{e}(\mathbf{u}_h) - \frac{1}{2}(\mathcal{C}^{-1}\boldsymbol{\sigma}_h + (\mathcal{C}^{-1}\boldsymbol{\sigma}_h)^{\mathrm{t}}))\boldsymbol{\nu}_T]\|_{[L^2(e)]^2}^2 \right\}^{1/2} \,\|\mathbf{v}\|_{[H^1(\Omega)]^2}, \qquad (41)
$$

and

$$
\left| \sum_{e \in E_h(\Omega)} \langle J[(\boldsymbol{\gamma}_h - \frac{1}{2}(\nabla \mathbf{u}_h - (\nabla \mathbf{u}_h)^{\mathrm{t}}))\boldsymbol{\nu}_T], \mathbf{v} - \mathbf{v}_h \rangle_{[L^2(e)]^2} \right|
$$

$$
\leq \sum_{e \in E_h(\Omega)} \| J[(\boldsymbol{\gamma}_h - \frac{1}{2}(\nabla \mathbf{u}_h - (\nabla \mathbf{u}_h)^{\mathrm{t}}))\boldsymbol{\nu}_T] \|_{[L^2(e)]^2} \| \mathbf{v} - \mathbf{v}_h \|_{[L^2(e)]^2}
$$

$$
\leq c_2 \sum_{e \in E_h(\Omega)} \| J[(\boldsymbol{\gamma}_h - \frac{1}{2}(\nabla \mathbf{u}_h - (\nabla \mathbf{u}_h)^{\mathrm{t}}))\boldsymbol{\nu}_T] \|_{[L^2(e)]^2} \, h_e^{1/2} \, \| \mathbf{v} \|_{[H^1(\Delta(e))]^2}
$$

$$
\leq C \left\{ \sum_{e \in E_h(\Omega)} h_e \| J[(\boldsymbol{\gamma}_h - \frac{1}{2}(\nabla \mathbf{u}_h - (\nabla \mathbf{u}_h)^{\mathrm{t}}))\boldsymbol{\nu}_T] \|_{[L^2(e)]^2}^2 \right\}^{1/2} \| \mathbf{v} \|_{[H^1(\Omega)]^2} . \tag{42}
$$

Therefore, placing (34)–(37) (resp. (39)–(42)) back into (29) and (30) (resp. (31) and (32)), employing the estimates (27), (28), and (33), and using the identities

$$
\sum_{e \in E_h(\Omega)} \int_e = \frac{1}{2} \sum_{T \in \mathcal{T}_h} \sum_{e \in E(T) \cap E_h(\Omega)} \int_e
$$

and

$$
\sum_{e \in E_h} \int_e = \sum_{e \in E_h(\Omega)} \int_e + \sum_{T \in \mathcal{T}_h} \sum_{e \in E(T) \cap E_h(\Gamma)} \int_e ,
$$

we conclude from (26) that

$$
\sup_{\substack{\mathbf{0} \neq (\boldsymbol{\tau}, \mathbf{v}, \boldsymbol{\eta}) \in \mathbf{H}_0 \\ \mathbf{div}\,(\boldsymbol{\tau}) = \mathbf{0}}} \frac{A((\boldsymbol{\sigma} - \boldsymbol{\sigma}_h, \mathbf{u} - \mathbf{u}_h, \boldsymbol{\gamma} - \boldsymbol{\gamma}_h), (\boldsymbol{\tau}, \mathbf{v}, \boldsymbol{\eta}))}{\| (\boldsymbol{\tau}, \mathbf{v}, \boldsymbol{\eta}) \|_{\mathbf{H}_0}} \leq C \, \boldsymbol{\theta} .
$$

This inequality and Lemma 3.1 complete the proof of reliability of $\boldsymbol{\theta}$.

We end this section by remarking that when the finite element subspace $\mathbf{H}_{0,h}$ is given by (16), that is when $\boldsymbol{\sigma}_h|_T \in [\mathbb{RT}_0(T)^{\mathrm{t}}]^2$, $\mathbf{u}_h|_T \in [\mathbb{P}_1(T)]^2$ and $\boldsymbol{\gamma}_h|_T \in [\mathbb{P}_0(T)]^{2 \times 2}$, then the expression (20) for θ_T^2 simplifies to

$$
\begin{aligned}
\theta_T^2 \;\; := \;\; & \| \mathbf{f} + \mathbf{div}\,(\boldsymbol{\sigma}_h) \|_{[L^2(T)]^2}^2 + \| \boldsymbol{\sigma}_h - \boldsymbol{\sigma}_h^{\mathrm{t}} \|_{[L^2(T)]^{2 \times 2}}^2 + \| \boldsymbol{\gamma}_h - \frac{1}{2}(\nabla \mathbf{u}_h - (\nabla \mathbf{u}_h)^{\mathrm{t}}) \|_{[L^2(T)]^{2 \times 2}}^2 \\
& + \; h_T^2 \left\{ \| \operatorname{curl}(\mathcal{C}^{-1}\boldsymbol{\sigma}_h) \|_{[L^2(T)]^2}^2 + \| \operatorname{curl}(\mathcal{C}^{-1}(\mathcal{C}^{-1}\boldsymbol{\sigma}_h)) \|_{[L^2(T)]^2}^2 \right\} \\
& + \sum_{e \in E(T)} h_e \left\{ \| J[(\mathcal{C}^{-1}\boldsymbol{\sigma}_h - \nabla \mathbf{u}_h + \boldsymbol{\gamma}_h)\mathbf{t}_T] \|_{[L^2(e)]^2}^2 + \| J[(\mathcal{C}^{-1}(\mathbf{e}(\mathbf{u}_h) - \mathcal{C}^{-1}\boldsymbol{\sigma}_h))\mathbf{t}_T] \|_{[L^2(e)]^2}^2 \right\} \\
& + \; h_T^2 \, \| \mathbf{div}\,(\frac{1}{2}(\mathcal{C}^{-1}\boldsymbol{\sigma}_h + (\mathcal{C}^{-1}\boldsymbol{\sigma}_h)^{\mathrm{t}})) \|_{[L^2(T)]^2}^2 \\
& + \sum_{e \in E(T) \cap E_h(\Omega)} h_e \, \| J[(\mathbf{e}(\mathbf{u}_h) - \frac{1}{2}(\mathcal{C}^{-1}\boldsymbol{\sigma}_h + (\mathcal{C}^{-1}\boldsymbol{\sigma}_h)^{\mathrm{t}}))\boldsymbol{\nu}_T] \|_{[L^2(e)]^2}^2 \\
& + \sum_{e \in E(T) \cap E_h(\Omega)} h_e \, \| J[(\boldsymbol{\gamma}_h - \frac{1}{2}(\nabla \mathbf{u}_h - (\nabla \mathbf{u}_h)^{\mathrm{t}}))\boldsymbol{\nu}_T] \|_{[L^2(e)]^2}^2 . \tag{43}
\end{aligned}
$$

4. Efficiency of the *a posteriori* error estimator

In this section we proceed as in [4] and [5] (see also [9]) and apply inverse inequalities (see [6]) and the localization technique introduced in [14], which is based on triangle-bubble and edge-bubble functions, to prove the efficiency of our *a posteriori* error estimator $\boldsymbol{\theta}$ (lower bound of the estimate (21)).

4.1. **Preliminaries**

We begin with some notations and preliminary results. Given $T \in \mathcal{T}_h$ and $e \in E(T)$, we let ψ_T and ψ_e be the usual triangle-bubble and edge-bubble functions, respectively (see (1.5) and (1.6) in [14]). In particular, ψ_T satisfies $\psi_T \in \mathbb{P}_3(T)$, $\mathrm{supp}(\psi_T) \subseteq T$, $\psi_T = 0$ on ∂T, and $0 \le \psi_T \le 1$ in T. Similarly, $\psi_e|_T \in \mathbb{P}_2(T)$, $\mathrm{supp}(\psi_e) \subseteq w_e := \cup\{T' \in \mathcal{T}_h : \quad e \in E(T')\}$, $\psi_e = 0$ on $\partial T\backslash e$, and $0 \le \psi_e \le 1$ in w_e. We also recall from [13] that, given $k \in \mathbb{N} \cup \{0\}$, there exists an extension operator $L : C(e) \to C(T)$ that satisfies $L(p) \in \mathbb{P}_k(T)$ and $L(p)|_e = p \; \forall p \in \mathbb{P}_k(e)$. Additional properties of ψ_T, ψ_e, and L are collected in the following lemma.

Lemma 4.1. *For any triangle T there exist positive constants c_1, c_2, c_3 and c_4, depending only on k and the shape of T, such that for all $q \in \mathbb{P}_k(T)$ and $p \in \mathbb{P}_k(e)$, there hold*

$$\|\psi_T \, q\|^2_{L^2(T)} \; \le \; \|q\|^2_{L^2(T)} \; \le \; c_1 \, \|\psi_T^{1/2} \, q\|^2_{L^2(T)} \,, \tag{44}$$

$$\|\psi_e \, p\|^2_{L^2(e)} \; \le \; \|p\|^2_{L^2(e)} \; \le \; c_2 \, \|\psi_e^{1/2} \, p\|^2_{L^2(e)} \,, \tag{45}$$

$$c_4 \, h_e \, \|p\|^2_{L^2(e)} \; \le \; \|\psi_e^{1/2} \, L(p)\|^2_{L^2(T)} \; \le \; c_3 \, h_e \, \|p\|^2_{L^2(e)} \,. \tag{46}$$

Proof. See Lemma 1.3 in [13]. $\qquad\qquad\square$

The following inverse estimate will also be used.

Lemma 4.2. *Let $l, m \in \mathbb{N} \cup \{0\}$ such that $l \le m$. Then, for any triangle T, there exists $c > 0$, depending only on k, l, m and the shape of T, such that*

$$|q|_{H^m(T)} \; \le \; c \, h_T^{l-m} \, |q|_{H^l(T)} \quad \forall \, q \in \mathbb{P}_k(T) \,. \tag{47}$$

Proof. See Theorem 3.2.6 in [6]. $\qquad\qquad\square$

Our goal is to estimate the 11 terms defining the error indicator θ_T^2 (*cf.* (20)). Using $\mathbf{f} = -\,\mathbf{div}\,\boldsymbol{\sigma}$, the symmetry of $\boldsymbol{\sigma}$, and $\boldsymbol{\gamma} = \frac{1}{2}(\nabla \mathbf{u} - (\nabla \mathbf{u})^{\mathrm{t}})$, we first observe that there hold

$$\|\mathbf{f} + \mathbf{div}\,(\boldsymbol{\sigma}_h)\|^2_{[L^2(T)]^2} \; = \; \|\,\mathbf{div}\,(\boldsymbol{\sigma} - \boldsymbol{\sigma}_h)\|^2_{[L^2(T)]^2} \,, \tag{48}$$

$$\|\boldsymbol{\sigma}_h - \boldsymbol{\sigma}_h^{\mathrm{t}}\|^2_{[L^2(T)]^{2\times 2}} \; \le \; 4 \, \|\boldsymbol{\sigma} - \boldsymbol{\sigma}_h\|^2_{[L^2(T)]^{2\times 2}} \,, \tag{49}$$

and

$$\|\boldsymbol{\gamma}_h - \frac{1}{2}(\nabla \mathbf{u}_h - (\nabla \mathbf{u}_h)^{\mathrm{t}})\|^2_{[L^2(T)]^{2\times 2}} \le 2 \left\{ \|\boldsymbol{\gamma} - \boldsymbol{\gamma}_h\|^2_{[L^2(T)]^{2\times 2}} + |\mathbf{u} - \mathbf{u}_h|^2_{[H^1(T)]^2} \right\}. \tag{50}$$

The upper bounds of the remaining 8 residual terms, which depend on the mesh parameters h_T and h_e, will be derived in Section 4.2 below. To this end we prove four lemmas establishing, in a sufficiently general way, some results concerning inverse inequalities and piecewise polynomials. They will be used to estimate the terms involving curl and $\mathbf{div}$ operators, and the normal and tangential jumps.

The result required for the curl operator is given first.

Lemma 4.3. *Let $\boldsymbol{\rho}_h \in [L^2(\Omega)]^{2\times 2}$ be a piecewise polynomial of degree $k \ge 0$ on each $T \in \mathcal{T}_h$. In addition, let $\boldsymbol{\rho} \in [L^2(\Omega)]^{2\times 2}$ be such that $\mathrm{curl}(\boldsymbol{\rho}) = \mathbf{0}$ on each $T \in \mathcal{T}_h$. Then, there exists $c > 0$, independent of h, such that for any $T \in \mathcal{T}_h$*

$$\|\,\mathrm{curl}(\boldsymbol{\rho}_h)\|_{[L^2(T)]^2} \; \le \; c \, h_T^{-1} \, \|\boldsymbol{\rho} - \boldsymbol{\rho}_h\|_{[L^2(T)]^{2\times 2}} \,. \tag{51}$$

Proof. We proceed as in the proof of Lemma 6.3 in [5]. Applying (44), integrating by parts, observing that $\psi_T = 0$ on ∂T, and using the Cauchy-Schwarz inequality, we obtain

$$c_1^{-1}\,\|\operatorname{curl}(\boldsymbol{\rho}_h)\|_{[L^2(T)]^2}^2 \;\leq\; \|\psi_T^{1/2}\,\operatorname{curl}(\boldsymbol{\rho}_h)\|_{[L^2(T)]^2}^2 \;=\; \int_T \psi_T\,\operatorname{curl}(\boldsymbol{\rho}_h)\cdot\operatorname{curl}(\boldsymbol{\rho}_h-\boldsymbol{\rho})$$

$$=\; \int_T (\boldsymbol{\rho}-\boldsymbol{\rho}_h):\underline{\mathbf{curl}}(\psi_T\operatorname{curl}(\boldsymbol{\rho}_h)) \;\leq\; \|\boldsymbol{\rho}-\boldsymbol{\rho}_h\|_{[L^2(T)]^{2\times2}}\,\|\underline{\mathbf{curl}}(\psi_T\operatorname{curl}(\boldsymbol{\rho}_h))\|_{[L^2(T)]^{2\times2}}. \tag{52}$$

Next, the inverse inequality (47) and the fact that $0 \leq \psi_T \leq 1$ give

$$\|\underline{\mathbf{curl}}(\psi_T\operatorname{curl}(\boldsymbol{\rho}_h))\|_{[L^2(T)]^{2\times2}} \;\leq\; c\,h_T^{-1}\,\|\psi_T\operatorname{curl}(\boldsymbol{\rho}_h)\|_{[L^2(T)]^2} \;\leq\; c\,h_T^{-1}\,\|\operatorname{curl}(\boldsymbol{\rho}_h)\|_{[L^2(T)]^2},$$

which, together with (52), yields (51). $\qquad\square$

The tangential jumps across the edges of the triangulation will be handled by employing the following estimate.

Lemma 4.4. *Let $\boldsymbol{\rho}_h \in [L^2(\Omega)]^{2\times2}$ be a piecewise polynomial of degree $k \geq 0$ on each $T \in \mathcal{T}_h$. Then, there exists $c > 0$, independent of h, such that for any $e \in E_h$*

$$\|J[\boldsymbol{\rho}_h\mathbf{t}_T]\|_{[L^2(e)]^2} \;\leq\; c\,h_e^{-1/2}\,\|\boldsymbol{\rho}_h\|_{[L^2(w_e)]^{2\times2}}. \tag{53}$$

Proof. Given an edge $e \in E_h$, we denote by $\mathbf{w}_h := J[\boldsymbol{\rho}_h\mathbf{t}_T]$ the corresponding tangential jump of $\boldsymbol{\rho}_h$. Then, employing (45) and integrating by parts on each triangle of w_e, we obtain

$$c_2^{-1}\,\|\mathbf{w}_h\|_{[L^2(e)]^2}^2 \;\leq\; \|\psi_e^{1/2}\,\mathbf{w}_h\|_{[L^2(e)]^2}^2 \;=\; \|\psi_e^{1/2}\,L(\mathbf{w}_h)\|_{[L^2(e)]^2}^2$$

$$=\; \int_e \psi_e\,L(\mathbf{w}_h)\cdot J[\boldsymbol{\rho}_h\mathbf{t}_T] \;=\; \int_{w_e} \operatorname{curl}(\boldsymbol{\rho}_h)\cdot\psi_e\,L(\mathbf{w}_h) \;+\; \int_{w_e} \boldsymbol{\rho}_h:\underline{\mathbf{curl}}(\psi_e L(\mathbf{w}_h)), \quad (54)$$

which, using the Cauchy-Schwarz inequality, yields

$$c_2^{-1}\,\|\mathbf{w}_h\|_{[L^2(e)]^2}^2 \;\leq\; \|\operatorname{curl}(\boldsymbol{\rho}_h)\|_{[L^2(w_e)]^2}\,\|\psi_e\,L(\mathbf{w}_h)\|_{[L^2(w_e)]^2}$$

$$+\;\; \|\boldsymbol{\rho}_h\|_{[L^2(w_e)]^{2\times2}}\,\|\underline{\mathbf{curl}}(\psi_e\,L(\mathbf{w}_h))\|_{[L^2(w_e)]^{2\times2}}. \tag{55}$$

Now, applying Lemma 4.3 with $\boldsymbol{\rho} = \mathbf{0}$ and using that $h_T^{-1} \leq h_e^{-1}$, we find that

$$\|\operatorname{curl}(\boldsymbol{\rho}_h)\|_{[L^2(w_e)]^2} \;\leq\; C\,h_e^{-1}\,\|\boldsymbol{\rho}_h\|_{[L^2(w_e)]^{2\times2}}. \tag{56}$$

On the other hand, employing (46) and the fact that $0 \leq \psi_e \leq 1$, we deduce that

$$\|\psi_e L(\mathbf{w}_h)\|_{[L^2(w_e)]^2} \;\leq\; C\,h_e^{1/2}\|\mathbf{w}_h\|_{[L^2(e)]^2}, \tag{57}$$

whereas the inverse estimate (47) and (46) yield

$$\|\underline{\mathbf{curl}}(\psi_e L(\mathbf{w}_h))\|_{[L^2(w_e)]^{2\times2}} \;\leq\; C\,h_e^{-1/2}\,\|\mathbf{w}_h\|_{[L^2(e)]^2}. \tag{58}$$

Finally, (53) follows easily from (55)–(58), which completes the proof. $\qquad\square$

The estimate required for the terms involving the **div** operator is provided next.

Lemma 4.5. *Let $\boldsymbol{\rho}_h \in [L^2(\Omega)]^{2\times 2}$ be a piecewise polynomial of degree $k \geq 0$ on each $T \in \mathcal{T}_h$. Then, there exists $c > 0$, independent of h, such that for any $T \in \mathcal{T}_h$*

$$\|\operatorname{\mathbf{div}}(\boldsymbol{\rho}_h)\|_{[L^2(T)]^2} \leq c\, h_T^{-1}\, \|\boldsymbol{\rho}_h\|_{[L^2(T)]^{2\times 2}}. \tag{59}$$

Proof. Applying (44), integrating by parts, and then employing the Cauchy-Schwarz inequality, we find that

$$
\begin{aligned}
c_1^{-1}\|\operatorname{\mathbf{div}}(\boldsymbol{\rho}_h)\|^2_{[L^2(T)]^2} &\leq \|\psi_T^{1/2}\operatorname{\mathbf{div}}(\boldsymbol{\rho}_h)\|^2_{[L^2(T)]^2} = \int_T \psi_T\,\operatorname{\mathbf{div}}(\boldsymbol{\rho}_h)\cdot\operatorname{\mathbf{div}}(\boldsymbol{\rho}_h)\\
&= -\int_T \boldsymbol{\rho}_h : \nabla(\psi_T\operatorname{\mathbf{div}}(\boldsymbol{\rho}_h)) \leq \|\boldsymbol{\rho}_h\|_{[L^2(T)]^{2\times 2}}\,\|\nabla(\psi_T\operatorname{\mathbf{div}}(\boldsymbol{\rho}_h))\|_{[L^2(T)]^{2\times 2}}.
\end{aligned}
\tag{60}
$$

Next, the inverse estimate (47) and the fact that $0 \leq \psi_T \leq 1$ in T imply that

$$\|\nabla(\psi_T\operatorname{\mathbf{div}}(\boldsymbol{\rho}_h))\|_{[L^2(T)]^{2\times 2}} \leq c\, h_T^{-1}\,\|\psi_T\operatorname{\mathbf{div}}(\boldsymbol{\rho}_h)\|_{[L^2(T)]^2} \leq c\, h_T^{-1}\,\|\operatorname{\mathbf{div}}(\boldsymbol{\rho}_h)\|_{[L^2(T)]^2},$$

which, together with (60), yields (59). $\qquad\square$

Finally, the estimate required for the normal jumps across the edges of the triangulation is established as follows.

Lemma 4.6. *Let $\boldsymbol{\rho}_h \in [L^2(\Omega)]^{2\times 2}$ be a piecewise polynomial of degree $k \geq 0$ on each $T \in \mathcal{T}_h$. Then, there exists $c > 0$, independent of h, such that for any $e \in E_h$*

$$\|J[\boldsymbol{\rho}_h\boldsymbol{\nu}_T]\|_{[L^2(e)]^2} \leq c\, h_e^{-1/2}\,\|\boldsymbol{\rho}_h\|_{[L^2(w_e)]^{2\times 2}}. \tag{61}$$

Proof. We proceed similarly as in the proof of Lemma 4.4. Given an edge $e \in E_h$, we now denote by $\mathbf{w}_h := J[\boldsymbol{\rho}_h\boldsymbol{\nu}_T]$ the corresponding normal jump of $\boldsymbol{\rho}_h$. Then, employing (45) and integrating by parts on each triangle of w_e, we obtain

$$
\begin{aligned}
c_2^{-1}\,\|\mathbf{w}_h\|^2_{[L^2(e)]^2} &\leq \|\psi_e^{1/2}\,\mathbf{w}_h\|^2_{[L^2(e)]^2} = \|\psi_e^{1/2}\,L(\mathbf{w}_h)\|^2_{[L^2(e)]^2}\\
&= \int_e \psi_e\,L(\mathbf{w}_h)\cdot J[\boldsymbol{\rho}_h\boldsymbol{\nu}_T] = \int_{w_e}\operatorname{\mathbf{div}}(\boldsymbol{\rho}_h)\cdot\psi_e\,L(\mathbf{w}_h) + \int_{w_e}\boldsymbol{\rho}_h : \nabla(\psi_e L(\mathbf{w}_h)),
\end{aligned}
\tag{62}
$$

which, using the Cauchy-Schwarz inequality, yields

$$
\begin{aligned}
c_2^{-1}\,\|\mathbf{w}_h\|^2_{[L^2(e)]^2} &\leq \|\operatorname{\mathbf{div}}(\boldsymbol{\rho}_h)\|_{[L^2(w_e)]^2}\,\|\psi_e\,L(\mathbf{w}_h)\|_{[L^2(w_e)]^2}\\
&\quad + \|\boldsymbol{\rho}_h\|_{[L^2(w_e)]^{2\times 2}}\,\|\nabla(\psi_e\,L(\mathbf{w}_h))\|_{[L^2(w_e)]^{2\times 2}}.
\end{aligned}
\tag{63}
$$

Now, applying Lemma 4.5 and using that $h_T^{-1} \leq h_e^{-1}$, we deduce that

$$\|\operatorname{\mathbf{div}}(\boldsymbol{\rho}_h)\|_{[L^2(w_e)]^2} \leq C\, h_e^{-1}\,\|\boldsymbol{\rho}_h\|_{[L^2(w_e)]^{2\times 2}}. \tag{64}$$

On the other hand, employing (46) and the fact that $0 \leq \psi_e \leq 1$, we deduce that

$$\|\psi_e L(\mathbf{w}_h)\|_{[L^2(w_e)]^2} \leq C\, h_e^{1/2}\|\mathbf{w}_h\|_{[L^2(e)]^2}, \tag{65}$$

whereas the inverse estimate (47) and (46) yield

$$\|\nabla(\psi_e L(\mathbf{w}_h))\|_{[L^2(w_e)]^{2\times 2}} \leq C\, h_e^{-1/2}\,\|\mathbf{w}_h\|_{[L^2(e)]^2}. \tag{66}$$

Finally, (61) follows easily from (63)–(66), which completes the proof. $\qquad\square$

We note that the generality of Lemmas 4.3–4.6 allows to apply them not only in the present context, but also in the *a posteriori* error analysis of other primal and mixed finite element methods.

4.2. **The main efficiency estimates**

As already announced, we now complete the proof of efficiency of $\boldsymbol{\theta}$ by conveniently applying Lemmas 4.3–4.6 to the corresponding terms defining θ_T^2.

Lemma 4.7. *There exist* C_1, $C_2 > 0$, *independent of* h *and* λ, *such that for any* $T \in \mathcal{T}_h$

$$h_T^2 \, \| \operatorname{curl}(\mathcal{C}^{-1}\boldsymbol{\sigma}_h + \boldsymbol{\gamma}_h)\|_{[L^2(T)]^2}^2 \leq C_1 \left\{ \|\boldsymbol{\sigma} - \boldsymbol{\sigma}_h\|_{[L^2(T)]^{2\times2}}^2 + \|\boldsymbol{\gamma} - \boldsymbol{\gamma}_h\|_{[L^2(T)]^{2\times2}}^2 \right\} \tag{67}$$

and

$$h_T^2 \, \| \operatorname{curl}(\mathcal{C}^{-1}(\mathbf{e}(\mathbf{u}_h) - \mathcal{C}^{-1}\boldsymbol{\sigma}_h))\|_{[L^2(T)]^2}^2 \leq C_2 \left\{ |\mathbf{u} - \mathbf{u}_h|_{[H^1(T)]^2}^2 + \|\boldsymbol{\sigma} - \boldsymbol{\sigma}_h\|_{[L^2(T)]^{2\times2}}^2 \right\}. \tag{68}$$

Proof. Applying Lemma 4.3 with $\boldsymbol{\rho}_h := \mathcal{C}^{-1}\boldsymbol{\sigma}_h + \boldsymbol{\gamma}_h$ and $\boldsymbol{\rho} := \nabla\mathbf{u} = \mathcal{C}^{-1}\boldsymbol{\sigma} + \boldsymbol{\gamma}$, and then using the triangle inequality and the continuity of $\mathcal{C}^{-1}$, we obtain

$$
\begin{aligned}
\| \operatorname{curl}(\mathcal{C}^{-1}\boldsymbol{\sigma}_h + \boldsymbol{\gamma}_h)\|_{[L^2(T)]^2} &\leq c \, h_T^{-1} \|(\mathcal{C}^{-1}\boldsymbol{\sigma} + \boldsymbol{\gamma}) - (\mathcal{C}^{-1}\boldsymbol{\sigma}_h + \boldsymbol{\gamma}_h)\|_{[L^2(T)]^{2\times2}} \\
&= c \, h_T^{-1} \|\mathcal{C}^{-1}(\boldsymbol{\sigma} - \boldsymbol{\sigma}_h) + (\boldsymbol{\gamma} - \boldsymbol{\gamma}_h)\|_{[L^2(T)]^{2\times2}} \\
&\leq C \, h_T^{-1} \left\{ \|\boldsymbol{\sigma} - \boldsymbol{\sigma}_h\|_{[L^2(T)]^{2\times2}} + \|\boldsymbol{\gamma} - \boldsymbol{\gamma}_h\|_{[L^2(T)]^{2\times2}} \right\},
\end{aligned}
$$

which yields (67). Similarly, (68) follows from Lemma 4.3 with $\boldsymbol{\rho}_h := \mathcal{C}^{-1}(\mathbf{e}(\mathbf{u}_h) - \mathcal{C}^{-1}\boldsymbol{\sigma}_h)$ and $\boldsymbol{\rho} := \mathcal{C}^{-1}(\mathbf{e}(\mathbf{u}) - \mathcal{C}^{-1}\boldsymbol{\sigma}) = \mathbf{0}$. $\qquad\square$

Lemma 4.8. *There exist* C_3, $C_4 > 0$, *independent of* h *and* λ, *such that for any* $e \in E_h$

$$
\begin{aligned}
&h_e \, J[(\mathcal{C}^{-1}\boldsymbol{\sigma}_h - \nabla\mathbf{u}_h + \boldsymbol{\gamma}_h)\mathbf{t}_T]\|_{[L^2(e)]^2}^2 \\
&\qquad \leq C_3 \left\{ \|\boldsymbol{\sigma} - \boldsymbol{\sigma}_h\|_{[L^2(w_e)]^{2\times2}}^2 + |\mathbf{u} - \mathbf{u}_h|_{[H^1(w_e)]^2}^2 + \|\boldsymbol{\gamma} - \boldsymbol{\gamma}_h\|_{[L^2(w_e)]^{2\times2}}^2 \right\}
\end{aligned}
\tag{69}
$$

and

$$h_e \, \|J[(\mathcal{C}^{-1}(\mathbf{e}(\mathbf{u}_h) - \mathcal{C}^{-1}\boldsymbol{\sigma}_h))\mathbf{t}_T]\|_{[L^2(e)]^2}^2 \leq C_4 \left\{ |\mathbf{u} - \mathbf{u}_h|_{[H^1(w_e)]^2}^2 + \|\boldsymbol{\sigma} - \boldsymbol{\sigma}_h\|_{[L^2(w_e)]^{2\times2}}^2 \right\}. \tag{70}$$

Proof. Applying Lemma 4.4 with $\boldsymbol{\rho}_h := \mathcal{C}^{-1}\boldsymbol{\sigma}_h - \nabla\mathbf{u}_h + \boldsymbol{\gamma}_h$, introducing $\mathbf{0} = \mathcal{C}^{-1}\boldsymbol{\sigma} - \nabla\mathbf{u} + \boldsymbol{\gamma}$ in the resulting estimate, and then using the triangle inequality and the continuity of $\mathcal{C}^{-1}$, we get

$$
\begin{aligned}
\|J[(\mathcal{C}^{-1}\boldsymbol{\sigma}_h - \nabla\mathbf{u}_h + \boldsymbol{\gamma}_h)\mathbf{t}_T]\|_{[L^2(e)]^2} &\leq c \, h_e^{-1/2} \|\mathcal{C}^{-1}\boldsymbol{\sigma}_h - \nabla\mathbf{u}_h + \boldsymbol{\gamma}_h\|_{[L^2(w_e)]^{2\times2}} \\
&= c \, h_e^{-1/2} \|\mathcal{C}^{-1}(\boldsymbol{\sigma}_h - \boldsymbol{\sigma}) + (\nabla\mathbf{u} - \nabla\mathbf{u}_h) + (\boldsymbol{\gamma}_h - \boldsymbol{\gamma})\|_{[L^2(w_e)]^{2\times2}} \\
&\leq C \, h_e^{-1/2} \left\{ \|\boldsymbol{\sigma} - \boldsymbol{\sigma}_h\|_{[L^2(w_e)]^{2\times2}} + |\mathbf{u} - \mathbf{u}_h|_{[H^1(w_e)]^2} + \|\boldsymbol{\gamma} - \boldsymbol{\gamma}_h\|_{[L^2(w_e)]^{2\times2}} \right\},
\end{aligned}
$$

which implies (69). Analogously, the estimate (70) is obtained from Lemma 4.4 defining $\boldsymbol{\rho}_h := \mathcal{C}^{-1}(\mathbf{e}(\mathbf{u}_h) - \mathcal{C}^{-1}\boldsymbol{\sigma}_h)$ and then introducing $\mathbf{0} = \mathcal{C}^{-1}(\mathbf{e}(\mathbf{u}) - \mathcal{C}^{-1}\boldsymbol{\sigma})$. $\qquad\square$

Lemma 4.9. *There exist* C_5, $C_6 > 0$, *independent of* h *and* λ, *such that for any* $T \in \mathcal{T}_h$

$$h_T^2 \, \|\operatorname{\mathbf{div}}(\mathbf{e}(\mathbf{u}_h) - \tfrac{1}{2}(\mathcal{C}^{-1}\boldsymbol{\sigma}_h + (\mathcal{C}^{-1}\boldsymbol{\sigma}_h)^{\mathbf{t}}))\|_{[L^2(T)]^2}^2 \leq C_5 \left\{ |\mathbf{u} - \mathbf{u}_h|_{[H^1(T)]^2}^2 + \|\boldsymbol{\sigma} - \boldsymbol{\sigma}_h\|_{[L^2(T)]^{2\times2}}^2 \right\} \tag{71}$$

and

$$h_T^2 \| \mathbf{div}\, (\boldsymbol{\gamma}_h - \frac{1}{2}(\nabla \mathbf{u}_h - (\nabla \mathbf{u}_h)^{\mathbf{t}})) \|_{[L^2(T)]^2}^2 \le C_6 \left\{ \| \boldsymbol{\gamma} - \boldsymbol{\gamma}_h \|_{[L^2(T)]^{2\times 2}}^2 + | \mathbf{u} - \mathbf{u}_h |_{[H^1(T)]^2}^2 \right\}. \qquad (72)$$

Proof. We apply Lemma 4.5 with $\boldsymbol{\rho}_h := \mathbf{e}(\mathbf{u}_h) - \frac{1}{2}(\mathcal{C}^{-1}\boldsymbol{\sigma}_h + (\mathcal{C}^{-1}\boldsymbol{\sigma}_h)^{\mathbf{t}})$, introduce the expression $\mathbf{0} = \mathbf{e}(\mathbf{u}) - \frac{1}{2}(\mathcal{C}^{-1}\boldsymbol{\sigma} + (\mathcal{C}^{-1}\boldsymbol{\sigma})^{\mathbf{t}})$ in the resulting estimate, and then use the triangle inequality and the continuity of the operators $\mathbf{e}$ and $\mathcal{C}^{-1}$, to obtain

$$\begin{aligned}
&\| \mathbf{div}\, (\mathbf{e}(\mathbf{u}_h) - \frac{1}{2}(\mathcal{C}^{-1}\boldsymbol{\sigma}_h + (\mathcal{C}^{-1}\boldsymbol{\sigma}_h)^{\mathbf{t}})) \|_{[L^2(T)]^2} \\
&\le c\, h_T^{-1} \| \mathbf{e}(\mathbf{u}_h) - \frac{1}{2}(\mathcal{C}^{-1}\boldsymbol{\sigma}_h + (\mathcal{C}^{-1}\boldsymbol{\sigma}_h)^{\mathbf{t}}) \|_{[L^2(T)]^{2\times 2}} \\
&= c\, h_T^{-1} \| (\mathbf{e}(\mathbf{u}_h) - \mathbf{e}(\mathbf{u})) + \frac{1}{2}(\mathcal{C}^{-1}(\boldsymbol{\sigma} - \boldsymbol{\sigma}_h) + (\mathcal{C}^{-1}(\boldsymbol{\sigma} - \boldsymbol{\sigma}_h))^{\mathbf{t}}) \|_{[L^2(T)]^{2\times 2}} \\
&\le C\, h_T^{-1} \left\{ | \mathbf{u} - \mathbf{u}_h |_{[H^1(T)]^2} + \| \boldsymbol{\sigma} - \boldsymbol{\sigma}_h \|_{[L^2(T)]^{2\times 2}} \right\},
\end{aligned}$$

which gives (71). Similarly, applying Lemma 4.5 with $\boldsymbol{\rho}_h := \boldsymbol{\gamma}_h - \frac{1}{2}(\nabla \mathbf{u}_h - (\nabla \mathbf{u}_h)^{\mathbf{t}})$ and introducing $\mathbf{0} = \boldsymbol{\gamma} - \frac{1}{2}(\nabla \mathbf{u} - (\nabla \mathbf{u})^{\mathbf{t}})$, we obtain (72). $\qquad \square$

Lemma 4.10. *There exist C_7, $C_8 > 0$, independent of h and λ, such that for any $e \in E_h$*

$$h_e \| J[(\mathbf{e}(\mathbf{u}_h) - \frac{1}{2}(\mathcal{C}^{-1}\boldsymbol{\sigma}_h + (\mathcal{C}^{-1}\boldsymbol{\sigma}_h)^{\mathbf{t}}))\boldsymbol{\nu}_T] \|_{[L^2(e)]^2}^2 \le C_7 \left\{ | \mathbf{u} - \mathbf{u}_h |_{[H^1(w_e)]^2}^2 + \| \boldsymbol{\sigma} - \boldsymbol{\sigma}_h \|_{[L^2(w_e)]^{2\times 2}}^2 \right\} \qquad (73)$$

and

$$h_e \| J[(\boldsymbol{\gamma}_h - \frac{1}{2}(\nabla \mathbf{u}_h - (\nabla \mathbf{u}_h)^{\mathbf{t}}))\boldsymbol{\nu}_T] \|_{[L^2(e)]^2}^2 \le C_8 \left\{ \| \boldsymbol{\gamma} - \boldsymbol{\gamma}_h \|_{[L^2(w_e)]^{2\times 2}}^2 + | \mathbf{u} - \mathbf{u}_h |_{[H^1(w_e)]^2}^2 \right\}. \qquad (74)$$

Proof. We apply Lemma 4.6 with $\boldsymbol{\rho}_h := \mathbf{e}(\mathbf{u}_h) - \frac{1}{2}(\mathcal{C}^{-1}\boldsymbol{\sigma}_h + (\mathcal{C}^{-1}\boldsymbol{\sigma}_h)^{\mathbf{t}})$, introduce the expression $\mathbf{0} := \mathbf{e}(\mathbf{u}) - \frac{1}{2}(\mathcal{C}^{-1}\boldsymbol{\sigma} + (\mathcal{C}^{-1}\boldsymbol{\sigma})^{\mathbf{t}})$, and then employ again the triangle inequality and the continuity of the operators $\mathbf{e}$ and $\mathcal{C}^{-1}$, to find that

$$\begin{aligned}
&\| J[(\mathbf{e}(\mathbf{u}_h) - \frac{1}{2}(\mathcal{C}^{-1}\boldsymbol{\sigma}_h + (\mathcal{C}^{-1}\boldsymbol{\sigma}_h)^{\mathbf{t}}))\boldsymbol{\nu}_T] \|_{[L^2(e)]^2} \\
&\le c\, h_e^{-1/2} \| \mathbf{e}(\mathbf{u}_h) - \frac{1}{2}(\mathcal{C}^{-1}\boldsymbol{\sigma}_h + (\mathcal{C}^{-1}\boldsymbol{\sigma}_h)^{\mathbf{t}}) \|_{[L^2(w_e)]^{2\times 2}} \\
&= c\, h_e^{-1/2} \| (\mathbf{e}(\mathbf{u}_h) - \mathbf{e}(\mathbf{u})) + \frac{1}{2}(\mathcal{C}^{-1}(\boldsymbol{\sigma} - \boldsymbol{\sigma}_h) + (\mathcal{C}^{-1}(\boldsymbol{\sigma} - \boldsymbol{\sigma}_h))^{\mathbf{t}}) \|_{[L^2(w_e)]^{2\times 2}} \\
&\le C\, h_e^{-1/2} \left\{ | \mathbf{u} - \mathbf{u}_h |_{[H^1(w_e)]^2} + \| \boldsymbol{\sigma} - \boldsymbol{\sigma}_h \|_{[L^2(w_e)]^{2\times 2}} \right\},
\end{aligned}$$

which yields (73). Analogously, the estimate (74) follows also from Lemma 4.6 defining $\boldsymbol{\rho}_h := \boldsymbol{\gamma}_h - \frac{1}{2}(\nabla \mathbf{u}_h + (\nabla \mathbf{u}_h)^{\mathbf{t}})$ and then introducing $\mathbf{0} = \boldsymbol{\gamma} - \frac{1}{2}(\nabla \mathbf{u} + (\nabla \mathbf{u})^{\mathbf{t}})$. $\qquad \square$

Finally, the efficiency of $\boldsymbol{\theta}$ (lower bound of (21)) follows straightforwardly from the estimates (48)–(50), (67), (68) (*cf.* Lem. 4.7), (69), (70) (*cf.* Lem. 4.8), (71), (72) (*cf.* Lem. 4.9), and (73), (74) (*cf.* Lem. 4.10), after summing over all $T \in \mathcal{T}_h$ and using that the number of triangles in each domain w_e is bounded by two.

5. NUMERICAL RESULTS

In this section we provide several numerical results illustrating the performance of the augmented mixed finite element scheme (10) and of the *a posteriori* error estimator $\boldsymbol{\theta}$ analyzed in this paper, using the specific finite element subspace $H_h^{\boldsymbol{\sigma}} \times H_{0,h}^{\mathbf{u}} \times H_h^{\boldsymbol{\gamma}}$, defined at the end of Section 2 (see (13)–(19)). We recall that in this case the local indicator θ_T^2 reduces to (43).

Now, before presenting the examples, we would like to remark in advance that, as compared with more traditional mixed methods, and besides the fact, already emphasized, of being able to choose any finite element subspace, our augmented approach presents other important advantages, as well. Indeed, let us first observe that in the case of uniform refinements each interior edge (resp. interior node) belongs to 2 (resp. 6) triangles, which yields corresponding correction factors of $\frac{1}{2}$ and $\frac{1}{6}$ when counting the global number of degrees of freedom, say N, in terms of the number of triangles, say M. Then, it is not difficult to see that the number of unknowns N of (10) behaves asymptotically as $5M$, whereas this behaviour is given by $7.5M$ when the well-known PEERS from [1] is used in the Galerkin scheme of the non-augmented formulation. In other words, the discrete system using PEERS introduces about 50% more degrees of freedom than our approach at each mesh, and therefore the augmented method becomes a much cheaper alternative. Furthermore, it is important to note that the polynomial degrees involved in the definition of $H_h^{\boldsymbol{\sigma}} \times H_{0,h}^{\mathbf{u}} \times H_h^{\boldsymbol{\gamma}}$, being 1, 1 and 0, yield simpler computations than for the PEERS subspace, whose polynomial degrees are 2, 0, and 1, respectively. Similarly, as compared with BDM (see *e.g.* [2, 3]), the augmented scheme also becomes more economical. In fact, as detailed for instance in [2], just the unknowns associated with the displacements and rotations of BDM are given by $6M$. To this amount, one still needs to add the degrees of freedom for the stresses which are given locally by a 15-dimensional space. Only after a static condensation process, BDM reduces to 6 unknowns per each edge, which yields N behaving as $9M$. Naturally, the competitive character of our augmented method has strongly motivated the need of deriving corresponding *a posteriori* error estimators in this paper. To this respect, and because of the introduction of the Galerkin-least squares terms needed to define the augmented formulation, we must recognize that $\boldsymbol{\theta}$ is certainly more expensive than, for instance, the error indicator introduced in [2]. However, it is also clear that the reliability and efficiency of $\boldsymbol{\theta}$ become more advantageous features than the sole reliability of the estimator in [2]. Finally, in connection with the residual-based *a posteriori* error estimator developed in [5] for PEERS and BDM, which is also reliable and efficient, we point out that the advantage of $\boldsymbol{\theta}$, though a bit more expensive, is still the freedom to choose the finite element subspaces defining the augmented scheme.

On the other hand, in order to implement the integral mean zero condition for functions of the space $H_{0,h}^{\boldsymbol{\sigma}} = \left\{\boldsymbol{\tau}_h \in H_h^{\boldsymbol{\sigma}} : \quad \int_\Omega tr(\boldsymbol{\tau}_h) = 0\right\}$ we introduce, as described in [10], a Lagrange multiplier ($\varphi_h \in \mathbb{R}$ below). That is, instead of (10), we consider the equivalent problem: Find $(\boldsymbol{\sigma}_h, \mathbf{u}_h, \boldsymbol{\gamma}_h, \varphi_h) \in H_h^{\boldsymbol{\sigma}} \times H_{0,h}^{\mathbf{u}} \times H_h^{\boldsymbol{\gamma}} \times \mathbb{R}$ such that

$$
\begin{aligned}
A((\boldsymbol{\sigma}_h, \mathbf{u}_h, \boldsymbol{\gamma}_h), (\boldsymbol{\tau}_h, \mathbf{v}_h, \boldsymbol{\eta}_h)) + \varphi_h \int_\Omega tr(\boldsymbol{\tau}_h) &= F(\boldsymbol{\tau}_h, \mathbf{v}_h, \boldsymbol{\eta}_h), \\
\psi_h \int_\Omega tr(\boldsymbol{\sigma}_h) &= 0,
\end{aligned}
\tag{75}
$$

for all $(\boldsymbol{\tau}_h, \mathbf{v}_h, \boldsymbol{\eta}_h, \psi_h) \in H_h^{\boldsymbol{\sigma}} \times H_{0,h}^{\mathbf{u}} \times H_h^{\boldsymbol{\gamma}} \times \mathbb{R}$. In fact, we recall from [10] the following theorem establishing the equivalence between (10) and (75).

Theorem 5.1.

a) *Let* $(\boldsymbol{\sigma}_h, \mathbf{u}_h, \boldsymbol{\gamma}_h) \in \mathbf{H}_{0,h}$ *be the solution of* (10). *Then* $(\boldsymbol{\sigma}_h, \mathbf{u}_h, \boldsymbol{\gamma}_h, 0)$ *is a solution of* (75).

b) *Let* $(\boldsymbol{\sigma}_h, \mathbf{u}_h, \boldsymbol{\gamma}_h, \varphi_h) \in H_h^{\boldsymbol{\sigma}} \times H_{0,h}^{\mathbf{u}} \times H_h^{\boldsymbol{\gamma}} \times \mathbb{R}$ *be a solution of* (75). *Then* $\varphi_h = 0$ *and* $(\boldsymbol{\sigma}_h, \mathbf{u}_h, \boldsymbol{\gamma}_h)$ *is the solution of* (10).

Proof. See Theorem 4.3 in [10]. □

In what follows, as indicated before, N stands for the total number of degrees of freedom (unknowns) of (75). Also, the individual and total errors are denoted by

$$e(\boldsymbol{\sigma}) := \|\boldsymbol{\sigma} - \boldsymbol{\sigma}_h\|_{H(\mathbf{div};\Omega)}, \quad e(\mathbf{u}) := |\mathbf{u} - \mathbf{u}_h|_{[H^1(\Omega)]^2}, \quad e(\boldsymbol{\gamma}) := \|\boldsymbol{\gamma} - \boldsymbol{\gamma}_h\|_{[L^2(\Omega)]^{2\times 2}},$$

and

$$e(\boldsymbol{\sigma}, \mathbf{u}, \boldsymbol{\gamma}) := \left\{ [e(\boldsymbol{\sigma})]^2 + [e(\mathbf{u})]^2 + [e(\boldsymbol{\gamma})]^2 \right\}^{1/2},$$

respectively, whereas the effectivity index with respect to $\boldsymbol{\theta}$ is defined by $e(\boldsymbol{\sigma}, \mathbf{u}, \boldsymbol{\gamma})/\boldsymbol{\theta}$.

On the other hand, we recall that given the Young modulus E and the Poisson ratio ν of a linear elastic material, the corresponding Lamé constants are defined by $\mu := \frac{E}{2(1+\nu)}$ and $\lambda := \frac{E\nu}{(1+\nu)(1-2\nu)}$. Then, in order to emphasize the robustness of the *a posteriori* error estimator $\boldsymbol{\theta}$ with respect to the Poisson ratio, in the examples below we fix $E = 1$ and consider $\nu = 0.4900$, $\nu = 0.4999$, or both, which yield the following values of μ and λ :

ν	μ	λ
0.4900	0.3356	16.4430
0.4999	0.3333	1666.4444

In addition, since the augmented method was already shown in [10] to be robust with respect to the parameters κ_1, κ_2, and κ_3, we simply consider for all the examples $(\kappa_1, \kappa_2, \kappa_3) = \left(\mu, \frac{1}{2\mu}, \frac{\mu}{2}\right)$, which corresponds to the feasible choice described in Theorem 2.1 with $\tilde{C}_1 = 1$ and $\tilde{C}_3 = \frac{1}{2}$.

We now specify the data of the five examples to be presented here. We take Ω as either the square $]0,1[^2$ or the L-shaped domain $]-0.5, 0.5[^2 \setminus [0, 0.5]^2$, and choose the datum $\mathbf{f}$ so that ν and the exact solution $\mathbf{u}(x_1, x_2) := (u_1(x_1, x_2), u_2(x_1, x_2))^{\mathrm{t}}$ are given in the table below. Actually, according to (1) and (2) we have $\boldsymbol{\sigma} = \lambda \operatorname{\mathbf{div}}(\mathbf{u})\,\mathbf{I} + 2\mu\,\mathbf{e}(\mathbf{u})$, and hence simple computations show that $\mathbf{f} := -\operatorname{\mathbf{div}}(\boldsymbol{\sigma}) = -(\lambda + \mu)\nabla(\operatorname{\mathbf{div}}\mathbf{u}) - \mu\,\Delta\,\mathbf{u}$. We also recall that the rotation $\boldsymbol{\gamma}$ is defined as $\frac{1}{2}\left(\nabla\mathbf{u} - (\nabla\mathbf{u})^{\mathrm{t}}\right)$.

We observe that the solution of Example 3 is singular at the boundary point $(0,0)$. In fact, the behaviour of $\mathbf{u}$ in a neighborhood of the origin implies that $\operatorname{\mathbf{div}}(\boldsymbol{\sigma}) \in [H^{1/3}(\Omega)]^2$ only, which, according to Theorem 2.3, yields $1/3$ as the expected rate of convergence for the uniform refinement. On the other hand, the solutions of Examples 1, 4, and 5 show large stress regions in a neighborhood of the boundary point $(1,1)$, in a neighborhood of the interior point $(1/2, 1/2)$, and around the line $x_1 = 0$, respectively.

EXAMPLE	Ω	ν	$u_1(x_1, x_2) = u_2(x_1, x_2)$
1	$]0, 1[^2$	0.4900	$\dfrac{x_1\,(x_1 - 1)\,x_2\,(x_2 - 1)}{(x_1 - 1)^2 + (x_2 - 1)^2 + 0.01}$
		0.4999	
2	$]0, 1[^2$	0.4900	$x_1\,(x_1 - 1)\,x_2\,(x_2 - 1)\,(x_1^2 + x_2^2)^{1/3}$
		0.4999	
3	$]-0.5, 0.5[^2 \setminus [0, 0.5]^2$	0.4900	$x_1\,x_2\,(x_1^2 - 0.25)\,(x_2^2 - 0.25)\,(x_1^2 + x_2^2)^{-1/3}$
4	$]0, 1[^2$	0.4900	$\dfrac{\sin(\pi\,x_1)\,\sin(\pi\,x_2)}{1000\,(x_1 - 1/2)^2 + 1000\,(x_2 - 1/2)^2 + 10}$
5	$]-0.5, 0.5[^2 \setminus [0, 0.5]^2$	0.4900	$x_1\,x_2\,(x_1^2 - 0.25)\,(x_2^2 - 0.25)\,(x_1^2 + 0.0001)^{-1/3}$

The numerical results given below were obtained using a *Compaq Alpha ES40 Parallel Computer* and a Fortran code. The linear system arising from the augmented mixed scheme (75) is implemented as explained in Section 4.3 of [10], and the individual errors are computed on each triangle using a Gaussian quadrature rule.

We first utilize Examples 1 and 2 to illustrate the good behaviour of the *a posteriori* error estimator $\boldsymbol{\theta}$ in a sequence of uniform meshes generated by equally spaced partitions on the sides of the square $]0,1[^2$. In Tables 5.1 through 5.4 we present the individual and total errors, the *a posteriori* error estimators, and the effectivity indices for these examples, with $\nu = 0.4900$ and $\nu = 0.4999$, for this sequence of uniform meshes. We remark that in both cases, and independently of how large the errors could become, there are practically no differences between the effectivity indices obtained with the two values of ν, which numerically shows the robustness of $\boldsymbol{\theta}$ with respect to the Poisson ratio (and hence with respect to the Lamé constant λ). Moreover, this index always remains in a neighborhood of 0.89 in Example 1 (resp. 0.46 in Ex. 2), which confirms the reliability and efficiency of $\boldsymbol{\theta}$. In fact, as established by our main Theorem 3.1, the effectivity index must lie between the constants $C_{\texttt{eff}}$ and $C_{\texttt{rel}}$ (see (21)).

Next, we consider Examples 3, 4, and 5, to illustrate the performance of the following adaptive algorithm based on $\boldsymbol{\theta}$ for the computation of the solutions of (75) (see [14]):

1. Start with a coarse mesh $\mathcal{T}_h$.
2. Solve the Galerkin scheme (75) for the current mesh $\mathcal{T}_h$.
3. Compute θ_T for each triangle $T \in \mathcal{T}_h$.
4. Consider stopping criterion and decide to finish or go to next step.
5. Use *blue-green* procedure to refine each element $T' \in \mathcal{T}_h$ whose local indicator $\theta_{T'}$ satisfies $\theta_{T'} \geq \frac{1}{2} \max\{\theta_T : \quad T \in \mathcal{T}_h\}$.
6. Define resulting mesh as the new $\mathcal{T}_h$ and go to step 2.

At this point we introduce the experimental rate of convergence, which, given two consecutive triangulations with degrees of freedom N and N' and corresponding total errors e and e', is defined by

$$r(e) := -2 \, \frac{\log(e/e')}{\log(N/N')} \cdot$$

In Tables 5.5 through 5.10 we provide the individual and total errors, the experimental rates of convergence, the *a posteriori* error estimators, and the effectivity indices for the uniform and adaptive refinements as applied to Examples 3–5. In this case, uniform refinement means that, given a uniform initial triangulation, each subsequent mesh is obtained from the previous one by dividing each triangle into the four ones arising when connecting the midpoints of its sides. We observe from these tables that the errors of the adaptive procedure decrease much faster than those obtained by the uniform one, which is confirmed by the experimental rates of convergence provided there. This fact can also be seen in Figures 5.1 through 5.3 where we display the total error $e(\boldsymbol{\sigma}, \mathbf{u}, \boldsymbol{\gamma})$ *vs.* the degrees of freedom N for both refinements. As shown by the values of $r(e)$, particularly in Example 3 (where $r(e)$ approaches $1/3$ for the uniform refinement), the adaptive method is able to recover, at least approximately, the quasi-optimal rate of convergence $O(h)$ for the total error. Furthermore, the effectivity indices remain again bounded from above and below, which confirms the reliability and efficiency of $\boldsymbol{\theta}$ for the adaptive algorithm. On the other hand, some intermediate meshes obtained with the adaptive refinement are displayed in Figures 5.4 through 5.6. Note that the method is able to recognize the singularities and the large stress regions of the solutions. In particular, this fact is observed in Example 3 (see Fig. 5.4) where the adapted meshes are highly refined around the singular point $(0,0)$. Similarly, the adapted meshes obtained in Examples 4 and 5 (see Figs. 5.5 and 5.6) concentrate the refinements around the interior point $(1/2, 1/2)$ and the segment $x_1 = 0$, respectively, where the largest stresses occur.

Summarizing, the numerical results presented in this section underline the reliability and efficiency of $\boldsymbol{\theta}$ and strongly demonstrate that the associated adaptive algorithm is much more suitable than a uniform discretization procedure when solving problems with non-smooth solutions.

TABLE 5.1. Mesh sizes, individual and total errors, *a posteriori* error estimators, and effectivity indices for a sequence of uniform meshes (Ex. 1, $\nu = 0.4900$).

N	h	$e(\boldsymbol{\sigma})$	$e(\mathbf{u})$	$e(\boldsymbol{\gamma})$	$e(\boldsymbol{\sigma}, \mathbf{u}, \boldsymbol{\gamma})$	$\boldsymbol{\theta}$	$e(\boldsymbol{\sigma}, \mathbf{u}, \boldsymbol{\gamma})/\boldsymbol{\theta}$
163	0.25000	0.9067E+2	0.2756E+1	0.1899E+1	0.9073E+2	0.1277E+3	0.7102
363	0.16667	0.9112E+2	0.2576E+1	0.2452E+1	0.9118E+2	0.1085E+3	0.8397
643	0.12500	0.7570E+2	0.2050E+1	0.2458E+1	0.7577E+2	0.8784E+2	0.8625
1003	0.10000	0.6100E+2	0.1673E+1	0.2321E+1	0.6107E+2	0.7070E+2	0.8637
1443	0.08333	0.5047E+2	0.1422E+1	0.2168E+1	0.5054E+2	0.5854E+2	0.8633
1963	0.07143	0.4348E+2	0.1227E+1	0.2026E+1	0.4355E+2	0.5026E+2	0.8663
2563	0.06250	0.3859E+2	0.1060E+1	0.1899E+1	0.3865E+2	0.4435E+2	0.8714
3243	0.05556	0.3483E+2	0.9191E+0	0.1784E+1	0.3489E+2	0.3980E+2	0.8766
4003	0.05000	0.3174E+2	0.8000E+0	0.1681E+1	0.3179E+2	0.3609E+2	0.8810
4843	0.04545	0.2911E+2	0.7009E+0	0.1587E+1	0.2916E+2	0.3297E+2	0.8846
5763	0.04167	0.2685E+2	0.6187E+0	0.1501E+1	0.2690E+2	0.3031E+2	0.8874
6763	0.03846	0.2489E+2	0.5503E+0	0.1423E+1	0.2494E+2	0.2803E+2	0.8898
7843	0.03571	0.2318E+2	0.4930E+0	0.1352E+1	0.2323E+2	0.2605E+2	0.8918
9003	0.03333	0.2169E+2	0.4446E+0	0.1286E+1	0.2173E+2	0.2432E+2	0.8936
10243	0.03125	0.2037E+2	0.4034E+0	0.1226E+1	0.2041E+2	0.2280E+2	0.8951
11563	0.02941	0.1919E+2	0.3681E+0	0.1171E+1	0.1923E+2	0.2145E+2	0.8965
12963	0.02777	0.1815E+2	0.3375E+0	0.1120E+1	0.1818E+2	0.2025E+2	0.8978

TABLE 5.2. Mesh sizes, individual and total errors, *a posteriori* error estimators, and effectivity indices for a sequence of uniform meshes (Ex. 1, $\nu = 0.4999$).

N	h	$e(\boldsymbol{\sigma})$	$e(\mathbf{u})$	$e(\boldsymbol{\gamma})$	$e(\boldsymbol{\sigma}, \mathbf{u}, \boldsymbol{\gamma})$	$\boldsymbol{\theta}$	$e(\boldsymbol{\sigma}, \mathbf{u}, \boldsymbol{\gamma})/\boldsymbol{\theta}$
163	0.25000	0.9045E+4	0.2534E+3	0.1713E+3	0.9050E+4	0.1257E+5	0.7198
363	0.16667	0.8986E+4	0.2439E+3	0.2248E+3	0.8992E+4	0.1065E+5	0.8446
643	0.12500	0.7447E+4	0.1962E+3	0.2268E+3	0.7453E+4	0.8609E+4	0.8657
1003	0.10000	0.5991E+4	0.1610E+3	0.2152E+3	0.5997E+4	0.6926E+4	0.8659
1443	0.08333	0.4948E+4	0.1372E+3	0.2019E+3	0.4954E+4	0.5729E+4	0.8647
1963	0.07143	0.4255E+4	0.1183E+3	0.1894E+3	0.4261E+4	0.4914E+4	0.8671
2563	0.06250	0.3771E+4	0.1022E+3	0.1781E+3	0.3777E+4	0.4332E+4	0.8719
3243	0.05556	0.3401E+4	0.8848E+2	0.1677E+3	0.3407E+4	0.3885E+4	0.8769
4003	0.05000	0.3098E+4	0.7688E+2	0.1583E+3	0.3103E+4	0.3521E+4	0.8813
4843	0.04545	0.2841E+4	0.6721E+2	0.1497E+3	0.2846E+4	0.3216E+4	0.8848
5763	0.04167	0.2620E+4	0.5918E+2	0.1418E+3	0.2625E+4	0.2957E+4	0.8877
6763	0.03846	0.2429E+4	0.5249E+2	0.1345E+3	0.2433E+4	0.2733E+4	0.8901
7843	0.03571	0.2262E+4	0.4688E+2	0.1279E+3	0.2266E+4	0.2540E+4	0.8922
9003	0.03333	0.2116E+4	0.4214E+2	0.1218E+3	0.2120E+4	0.2371E+4	0.8940
10243	0.03125	0.1987E+4	0.3810E+2	0.1162E+3	0.1991E+4	0.2223E+4	0.8956
11563	0.02941	0.1873E+4	0.3462E+2	0.1110E+3	0.1876E+4	0.2092E+4	0.8970
12963	0.02777	0.1771E+4	0.3161E+2	0.1062E+3	0.1774E+4	0.1975E+4	0.8983

TABLE 5.3. Mesh sizes, individual and total errors, *a posteriori* error estimators, and effectivity indices for a sequence of uniform meshes (Ex. 2, $\nu = 0.4900$).

N	h	$e(\boldsymbol{\sigma})$	$e(\mathbf{u})$	$e(\boldsymbol{\gamma})$	$e(\boldsymbol{\sigma},\mathbf{u},\boldsymbol{\gamma})$	$\boldsymbol{\theta}$	$e(\boldsymbol{\sigma},\mathbf{u},\boldsymbol{\gamma})/\boldsymbol{\theta}$
163	0.25000	0.2730E+1	0.1483E+0	0.2631E+0	0.2747E+1	0.8203E+1	0.3349
363	0.16666	0.1841E+1	0.1108E+0	0.2492E+0	0.1861E+1	0.5159E+1	0.3607
643	0.12500	0.1386E+1	0.8231E-1	0.2236E+0	0.1406E+1	0.3696E+1	0.3804
1003	0.10000	0.1110E+1	0.6260E-1	0.1978E+0	0.1129E+1	0.2855E+1	0.3955
1443	0.08333	0.9259E+0	0.4904E-1	0.1751E+0	0.9436E+0	0.2315E+1	0.4074
1963	0.07143	0.7939E+0	0.3952E-1	0.1561E+0	0.8101E+0	0.1941E+1	0.4171
2563	0.06250	0.6947E+0	0.3264E-1	0.1403E+0	0.7095E+0	0.1668E+1	0.4252
3243	0.05556	0.6176E+0	0.2753E-1	0.1271E+0	0.6311E+0	0.1460E+1	0.4320
4003	0.05000	0.5558E+0	0.2364E-1	0.1160E+0	0.5683E+0	0.1297E+1	0.4378
4843	0.04545	0.5053E+0	0.2061E-1	0.1066E+0	0.5169E+0	0.1166E+1	0.4429
5763	0.04167	0.4632E+0	0.1820E-1	0.9852E-1	0.4739E+0	0.1059E+1	0.4474
6763	0.03846	0.4276E+0	0.1626E-1	0.9153E-1	0.4376E+0	0.9695E+0	0.4513
7843	0.03571	0.3970E+0	0.1466E-1	0.8543E-1	0.4064E+0	0.8935E+0	0.4548
9003	0.03333	0.3706E+0	0.1333E-1	0.8006E-1	0.3794E+0	0.8284E+0	0.4579
10243	0.03125	0.3474E+0	0.1221E-1	0.7532E-1	0.3557E+0	0.7719E+0	0.4608
11563	0.02941	0.3270E+0	0.1126E-1	0.7109E-1	0.3348E+0	0.7226E+0	0.4633
12963	0.02777	0.3088E+0	0.1044E-1	0.6730E-1	0.3162E+0	0.6791E+0	0.4657

TABLE 5.4. Mesh sizes, individual and total errors, *a posteriori* error estimators, and effectivity indices for a sequence of uniform meshes (Ex. 2, $\nu = 0.4999$).

N	h	$e(\boldsymbol{\sigma})$	$e(\mathbf{u})$	$e(\boldsymbol{\gamma})$	$e(\boldsymbol{\sigma},\mathbf{u},\boldsymbol{\gamma})$	$\boldsymbol{\theta}$	$e(\boldsymbol{\sigma},\mathbf{u},\boldsymbol{\gamma})/\boldsymbol{\theta}$
163	0.25000	0.2707E+3	0.1356E+2	0.2536E+2	0.2722E+3	0.8067E+3	0.3374
363	0.16666	0.1825E+3	0.1053E+2	0.2375E+2	0.1843E+3	0.5070E+3	0.3635
643	0.12500	0.1373E+3	0.7847E+1	0.2126E+2	0.1392E+3	0.3628E+3	0.3837
1003	0.10000	0.1100E+3	0.5913E+1	0.1879E+2	0.1118E+3	0.2801E+3	0.3990
1443	0.08333	0.9176E+2	0.4558E+1	0.1665E+2	0.9337E+2	0.2270E+3	0.4112
1963	0.07143	0.7867E+2	0.3599E+1	0.1484E+2	0.8014E+2	0.1903E+3	0.4211
2563	0.06250	0.6884E+2	0.2903E+1	0.1334E+2	0.7018E+2	0.1634E+3	0.4293
3243	0.05556	0.6119E+2	0.2386E+1	0.1209E+2	0.6242E+2	0.1430E+3	0.4362
4003	0.05000	0.5507E+2	0.1993E+1	0.1104E+2	0.5620E+2	0.1270E+3	0.4422
4843	0.04545	0.5007E+2	0.1689E+1	0.1014E+2	0.5111E+2	0.1142E+3	0.4474
5763	0.04167	0.4589E+2	0.1449E+1	0.9377E+1	0.4686E+2	0.1036E+3	0.4519
6763	0.03846	0.4236E+2	0.1256E+1	0.8712E+1	0.4327E+2	0.9490E+2	0.4559
7843	0.03571	0.3934E+2	0.1099E+1	0.8132E+1	0.4018E+2	0.8745E+2	0.4595
9003	0.03333	0.3671E+2	0.9697E+0	0.7622E+1	0.3751E+2	0.8106E+2	0.4627
10243	0.03125	0.3442E+2	0.8617E+0	0.7171E+1	0.3517E+2	0.7553E+2	0.4656
11563	0.02941	0.3239E+2	0.7708E+0	0.6768E+1	0.3310E+2	0.7070E+2	0.4682
12963	0.02777	0.3059E+2	0.6935E+0	0.6408E+1	0.3126E+2	0.6644E+2	0.4706

TABLE 5.5. Individual and total errors, experimental rates of convergence, *a posteriori* error estimators, and effectivity indices for the uniform refinement (Ex. 3).

N	$e(\boldsymbol{\sigma})$	$e(\mathbf{u})$	$e(\boldsymbol{\gamma})$	$e(\boldsymbol{\sigma}, \mathbf{u}, \boldsymbol{\gamma})$	$r(e)$	$\boldsymbol{\theta}$	$e(\boldsymbol{\sigma}, \mathbf{u}, \boldsymbol{\gamma})/\boldsymbol{\theta}$
123	0.2182E+1	0.1994E+0	0.9131E-1	0.2193E+1	——	0.2898E+1	0.7567
483	0.1525E+1	0.9385E-1	0.9919E-1	0.1531E+1	0.5254	0.1840E+1	0.8323
1923	0.1122E+1	0.4040E-1	0.7723E-1	0.1125E+1	0.4455	0.1242E+1	0.9058
7683	0.8585E+0	0.2246E-1	0.4795E-1	0.8601E+0	0.3885	0.8996E+0	0.9561

TABLE 5.6. Individual and total errors, experimental rates of convergence, *a posteriori* error estimators, and effectivity indices for the adaptive refinement (Ex. 3).

| N	$e(\boldsymbol{\sigma})$	$e(\mathbf{u})$	$e(\boldsymbol{\gamma})$	$e(\boldsymbol{\sigma}, \mathbf{u}, \boldsymbol{\gamma})$	$r(e)$	$\boldsymbol{\theta}$	$e(\boldsymbol{\sigma}, \mathbf{u}, \boldsymbol{\gamma})/\boldsymbol{\theta}$
123	0.2182E+1	0.1994E+0	0.9131E-1	0.2193E+1	——	0.2898E+1	0.7567
243	0.1795E+1	0.1516E+0	0.7951E-1	0.1803E+1	0.5745	0.2340E+1	0.7707
483	0.1372E+1	0.9211E-1	0.8634E-1	0.1378E+1	0.7839	0.1702E+1	0.8094
543	0.1259E+1	0.9159E-1	0.8658E-1	0.1265E+1	1.4583	0.1609E+1	0.7860
663	0.1137E+1	0.8250E-1	0.8357E-1	0.1143E+1	1.0150	0.1476E+1	0.7746
778	0.1045E+1	0.8113E-1	0.8228E-1	0.1051E+1	1.0454	0.1386E+1	0.7583
1228	0.8540E+0	0.7469E-1	0.6693E-1	0.8599E+0	0.8821	0.1100E+1	0.7814
1518	0.7810E+0	0.7270E-1	0.5604E-1	0.7864E+0	0.8423	0.9562E+0	0.8224
1783	0.7100E+0	0.7233E-1	0.6058E-1	0.7162E+0	1.1622	0.8812E+0	0.8127
2288	0.6381E+0	0.7912E-1	0.6245E-1	0.6460E+0	0.8269	0.7869E+0	0.8209
2533	0.6040E+0	0.7605E-1	0.6008E-1	0.6117E+0	1.0727	0.7569E+0	0.8082
3663	0.5089E+0	0.9206E-1	0.5993E-1	0.5206E+0	0.8745	0.6383E+0	0.8156
4703	0.4449E+0	0.7418E-1	0.5634E-1	0.4546E+0	1.0850	0.5560E+0	0.8175
5698	0.4056E+0	0.7651E-1	0.5628E-1	0.4166E+0	0.9091	0.5052E+0	0.8246
7243	0.3654E+0	0.7278E-1	0.5394E-1	0.3764E+0	0.8448	0.4506E+0	0.8355
8203	0.3428E+0	0.6653E-1	0.5370E-1	0.3533E+0	1.0209	0.4290E+0	0.8234
10818	0.3138E+0	0.8197E-1	0.5696E-1	0.3293E+0	0.5078	0.3865E+0	0.8520
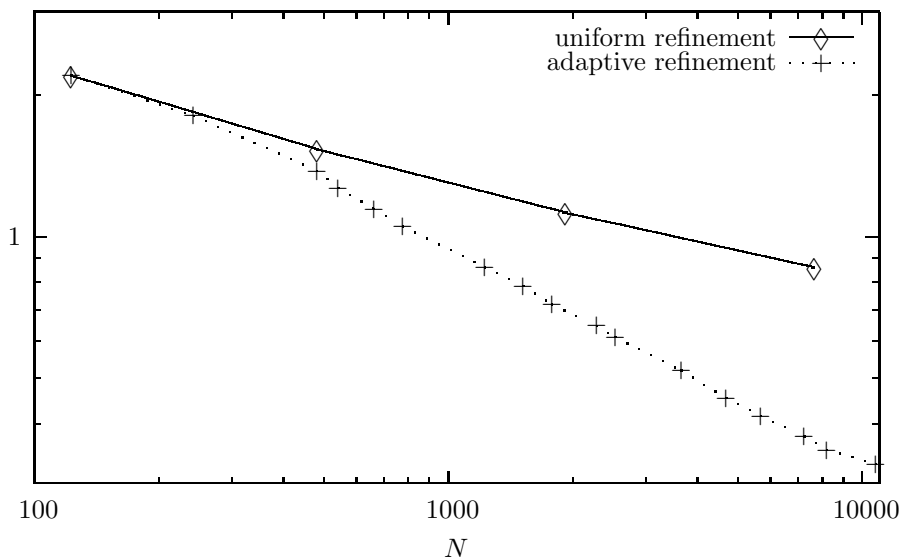
FIGURE 5.1. Total errors $e(\boldsymbol{\sigma}, \mathbf{u}, \boldsymbol{\gamma})$ *vs.* degrees of freedom N for the uniform and adaptive refinements (Ex. 3).

TABLE 5.7. Individual and total errors, experimental rates of convergence, *a posteriori* error estimators, and effectivity indices for the uniform refinement (Ex. 4).

N	$e(\boldsymbol{\sigma})$	$e(\mathbf{u})$	$e(\boldsymbol{\gamma})$	$e(\boldsymbol{\sigma},\mathbf{u},\boldsymbol{\gamma})$	$r(e)$	$\boldsymbol{\theta}$	$e(\boldsymbol{\sigma},\mathbf{u},\boldsymbol{\gamma})/\boldsymbol{\theta}$
163	0.3813E+2	0.5025E+1	0.2685E+1	0.3855E+2	——	0.4070E+2	0.9472
643	0.3593E+2	0.2015E+1	0.1361E+1	0.3601E+2	0.0991	0.3692E+2	0.9755
2563	0.2021E+2	0.1035E+1	0.8087E+0	0.2025E+2	0.8327	0.2093E+2	0.9673
10243	0.9898E+1	0.7493E+0	0.6000E+0	0.9944E+1	1.0267	0.1027E+2	0.9677

TABLE 5.8. Individual and total errors, experimental rates of convergence, *a posteriori* error estimators, and effectivity indices for the adaptive refinement (Ex. 4).

N	$e(\boldsymbol{\sigma})$	$e(\mathbf{u})$	$e(\boldsymbol{\gamma})$	$e(\boldsymbol{\sigma},\mathbf{u},\boldsymbol{\gamma})$	$r(e)$	$\boldsymbol{\theta}$	$e(\boldsymbol{\sigma},\mathbf{u},\boldsymbol{\gamma})/\boldsymbol{\theta}$
163	0.3813E+2	0.5025E+1	0.2685E+1	0.3855E+2	——	0.4070E+2	0.9472
343	0.3594E+2	0.1913E+1	0.1156E+1	0.3601E+2	0.1827	0.3686E+2	0.9771
643	0.2042E+2	0.1255E+1	0.8721E+0	0.2048E+2	1.7958	0.2122E+2	0.9654
883	0.1174E+2	0.1232E+1	0.6751E+0	0.1183E+2	3.4620	0.1237E+2	0.9559
2583	0.6525E+1	0.1246E+1	0.7400E+0	0.6684E+1	1.0638	0.7092E+1	0.9424
4988	0.4748E+1	0.1109E+1	0.6405E+0	0.4918E+1	0.9324	0.5114E+1	0.9615
9748	0.3540E+1	0.8796E+0	0.5435E+0	0.3688E+1	0.8591	0.3785E+1	0.9743
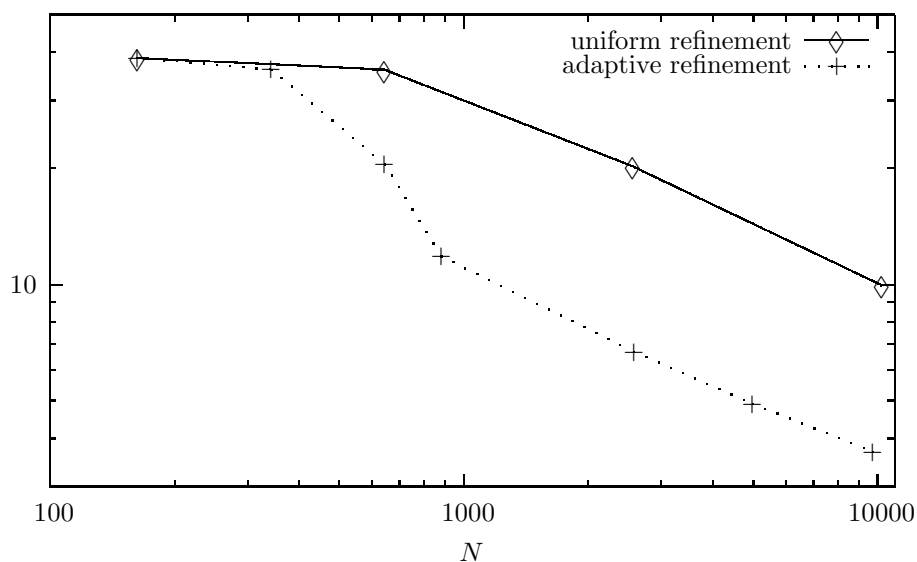
FIGURE 5.2. Total errors $e(\boldsymbol{\sigma},\mathbf{u},\boldsymbol{\gamma})$ *vs.* degrees of freedom N for the uniform and adaptive refinements (Ex. 4).

TABLE 5.9. Individual and total errors, experimental rates of convergence, *a posteriori* error estimators, and effectivity indices for the uniform refinement (Ex. 5).

N	$e(\boldsymbol{\sigma})$	$e(\mathbf{u})$	$e(\boldsymbol{\gamma})$	$e(\boldsymbol{\sigma}, \mathbf{u}, \boldsymbol{\gamma})$	$r(e)$	$\boldsymbol{\theta}$	$e(\boldsymbol{\sigma}, \mathbf{u}, \boldsymbol{\gamma})/\boldsymbol{\theta}$
123	0.1399E+2	0.4737E+0	0.1629E+0	0.1400E+2	——	0.1436E+2	0.9745
483	0.2522E+2	0.2957E+0	0.1577E+0	0.2522E+2	——	0.2527E+2	0.9980
1923	0.2494E+2	0.1375E+0	0.1454E+0	0.2494E+2	0.0162	0.2496E+2	0.9992
7683	0.1449E+2	0.6395E-1	0.1742E+0	0.1449E+2	0.7834	0.1453E+2	0.9975

TABLE 5.10. Individual and total errors, experimental rates of convergence, *a posteriori* error estimators, and effectivity indices for the adaptive refinement (Ex. 5).

N	$e(\boldsymbol{\sigma})$	$e(\mathbf{u})$	$e(\boldsymbol{\gamma})$	$e(\boldsymbol{\sigma}, \mathbf{u}, \boldsymbol{\gamma})$	$r(e)$	$\boldsymbol{\theta}$	$e(\boldsymbol{\sigma}, \mathbf{u}, \boldsymbol{\gamma})/\boldsymbol{\theta}$
123	0.1399E+2	0.4737E+0	0.1629E+0	0.1400E+2	——	0.1436E+2	0.9745
263	0.2524E+2	0.3215E+0	0.1510E+0	0.2524E+2	——	0.2535E+2	0.9957
513	0.2498E+2	0.2298E+0	0.1420E+0	0.2498E+2	0.0309	0.2507E+2	0.9963
988	0.1507E+2	0.2026E+0	0.1888E+0	0.1507E+2	1.5421	0.1523E+2	0.9894
2383	0.8488E+1	0.1927E+0	0.1773E+0	0.8492E+1	1.3033	0.8603E+1	0.9871
4038	0.6955E+1	0.1424E+0	0.1249E+0	0.6958E+1	0.7556	0.7042E+1	0.9881
7938	0.5361E+1	0.1458E+0	0.1082E+0	0.5364E+1	0.7696	0.5439E+1	0.9862
12743	0.4272E+1	0.1353E+0	0.1044E+0	0.4275E+1	0.9587	0.4331E+1	0.9870
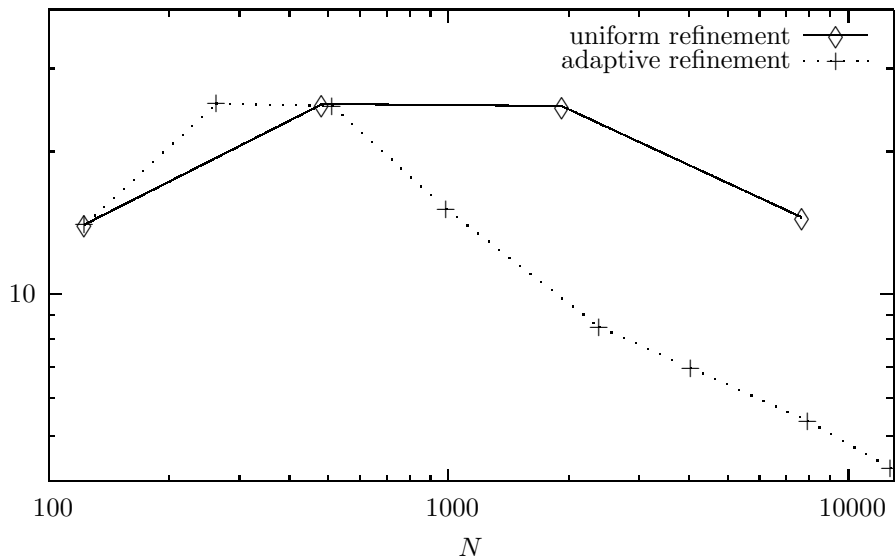
FIGURE 5.3. Total errors $e(\boldsymbol{\sigma}, \mathbf{u}, \boldsymbol{\gamma})$ *vs.* degrees of freedom N for the uniform and adaptive refinements (Ex. 5).
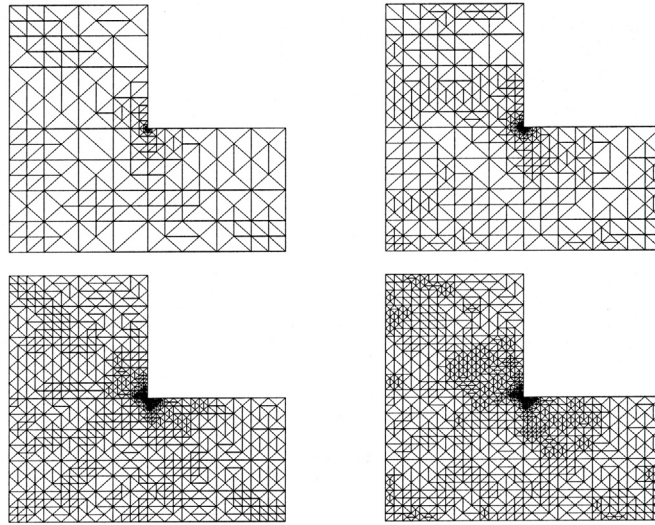
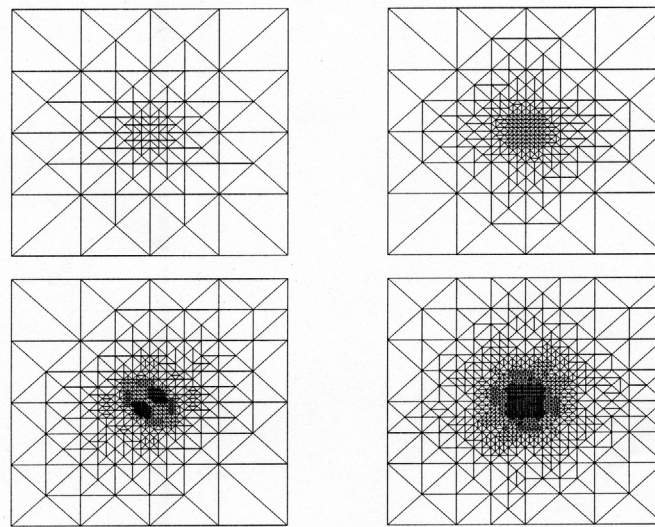FIGURE 5.4. Adapted intermediate meshes with 1783, 3663, 8203, and 10 818 degrees of freedom (Ex. 3).

FIGURE 5.5. Adapted intermediate meshes with 883, 2583, 4988, and 9748 degrees of freedom (Ex. 4).
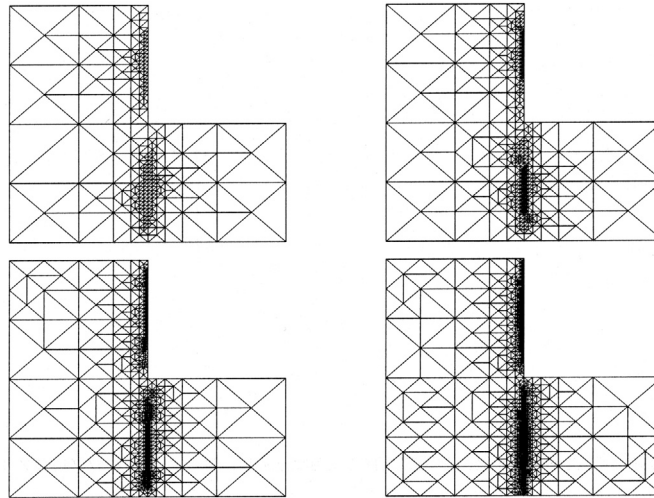
FIGURE 5.6. Adapted intermediate meshes with 2383, 4038, 7938, and 12 743 degrees of freedom (Ex. 5).

REFERENCES

[1] D.N. Arnold, F. Brezzi and J. Douglas, PEERS: A new mixed finite element method for plane elasticity. *Japan J. Appl. Math.* **1** (1984) 347–367.

[2] D. Braess, O. Klaas, R. Niekamp, E. Stein and F. Wobschal, Error indicators for mixed finite elements in 2-dimensional linear elasticity. *Comput. Method. Appl. M.* **127** (1995) 345–356.

[3] F. Brezzi and M. Fortin, *Mixed and Hybrid Finite Element Methods.* Springer-Verlag (1991).

[4] C. Carstensen, *A posteriori* error estimate for the mixed finite element method. *Math. Comput.* **66** (1997) 465–476.

[5] C. Carstensen and G. Dolzmann, *A posteriori* error estimates for mixed FEM in elasticity. *Numer. Math.* **81** (1998) 187–209.

[6] P.G. Ciarlet, *The Finite Element Method for Elliptic Problems.* North-Holland, Amsterdam, New York, Oxford (1978).

[7] P. Clément, Approximation by finite element functions using local regularisation. *RAIRO Anal. Numér.* **9** (1975) 77–84.

[8] J. Douglas and J. Wan, An absolutely stabilized finite element method for the Stokes problem. *Math. Comput.* **52** (1989) 495–508.

[9] G.N. Gatica, A note on the efficiency of residual-based *a posteriori* error estimators for some mixed finite element methods. *Electronic Trans. Numer. Anal.* **17** (2004) 218–233.

[10] G.N. Gatica, Analysis of a new augmented mixed finite element method for linear elasticity allowing $\mathbb{RT}_0 - \mathbb{P}_1 - \mathbb{P}_0$ approximations. *ESAIM: M2AN* **40** (2006) 1–28.

[11] A. Masud and T.J.R. Hughes, A stabilized mixed finite element method for Darcy flow. *Comput. Method. Appl. M.* **191** (2002) 4341–4370.

[12] J.E. Roberts and J.-M. Thomas, Mixed and Hybrid Methods, in *Handbook of Numerical Analysis* **II**, Finite Element Methods (Part 1) P.G. Ciarlet and J.L. Lions Eds., North-Holland, Amsterdam (1991).

[13] R. Verfürth, *A posteriori* error estimation and adaptive mesh-refinement techniques. *J. Comput. Appl. Math.* **50** (1994) 67–83.

[14] R. Verfürth, *A Review of A Posteriori Error Estimation and Adaptive Mesh-Refinement Techniques.* Wiley-Teubner (Chichester) (1996).